Observed Vegetation–Climate Feedbacks in the United States*

M. NOTARO AND Z. LIU

Center for Climatic Research, University of Wisconsin—Madison, Madison, Wisconsin

J. W. WILLIAMS

Department of Geography, University of Wisconsin—Madison, Madison, Wisconsin

(Manuscript submitted 4 February 2005, in final form 3 August 2005)

ABSTRACT

Observed vegetation feedbacks on temperature and precipitation are assessed across the United States using satellite-based fraction of photosynthetically active radiation (FPAR) and monthly climate data for the period of 1982–2000. This study represents the first attempt to spatially quantify the observed local impact of vegetation on temperature and precipitation over the United States for all months and by season. Lead–lag correlations and feedback parameters are computed to determine the regions where vegetation substantially impacts the atmosphere and to quantify this forcing. Temperature imposes a significant instantaneous forcing on FPAR, while precipitation's impact on FPAR is greatest at one-month lead, particularly across the prairie. An increase in vegetation raises the surface air temperature by absorbing additional radiation and, in some cases, masking the high albedo of snow cover. Vegetation generally exhibits a positive forcing on temperature, strongest in spring and particularly across the northern states. The local impact of FPAR on precipitation appears to be spatially inhomogeneous and relatively weak, potentially due to the atmospheric transport of transpired water. The computed feedback parameters can be used to evaluate vegetation–climate interactions simulated by models with dynamic vegetation.

1. Introduction

Vegetation and climate interact through a series of complex feedbacks, which are not yet fully understood. Patterns of natural vegetation are largely determined by temperature, precipitation, solar irradiance, soil conditions, and CO_2 concentration (Budyko 1974; Woodward 1987; Woodward et al. 2004). Vegetation impacts climate directly through moisture, energy, and momentum exchanges with the atmosphere and indirectly through biogeochemical processes that alter atmospheric CO_2 concentration (Pielke et al. 1998; Bonan 2002). The key vegetation–climate feedbacks are outlined in Fig. 1.

Plants regulate evapotranspiration by adjusting the size of their stomatal openings (Shukla and Mintz 1982; Jones 1983; Henderson-Sellers et al. 1995; Pollard and Thompson 1995; Bonan 2002). Through this moisture feedback, an increase in evapotranspiration potentially leads to an increase in atmospheric column moisture and precipitation, further enhancing plant growth. Changes in vegetation alter the surface albedo and radiation fluxes, leading to a local temperature change and eventually a vegetation response. This albedo (energy) feedback is particularly important when forests mask snow cover and grass spreads into desert (Robinson and Kukla 1985; Bonan et al. 1992; Betts and Ball 1997; Bonan 2002). Through the momentum feedback, variations in the surface roughness of vegetation alter wind speeds, moisture convergence, turbulence, and the depth of the atmospheric boundary layer, which then affect vegetation growth (Sud et al. 1988; Buermann 2002).

Most of the current understanding of these feedbacks resulted from studies using coupled vegetation–climate models. Foley et al. (1998) found that the northward expansion of grasslands in an interactive vegetation simulation of the Global Environmental and Ecological

* CCR Contribution Number 896.

Corresponding author address: Michael Notaro, Center for Climatic Research, 1225 West Dayton Street, Rm. 1103, Madison, WI 53706.
E-mail: mnotaro@wisc.edu

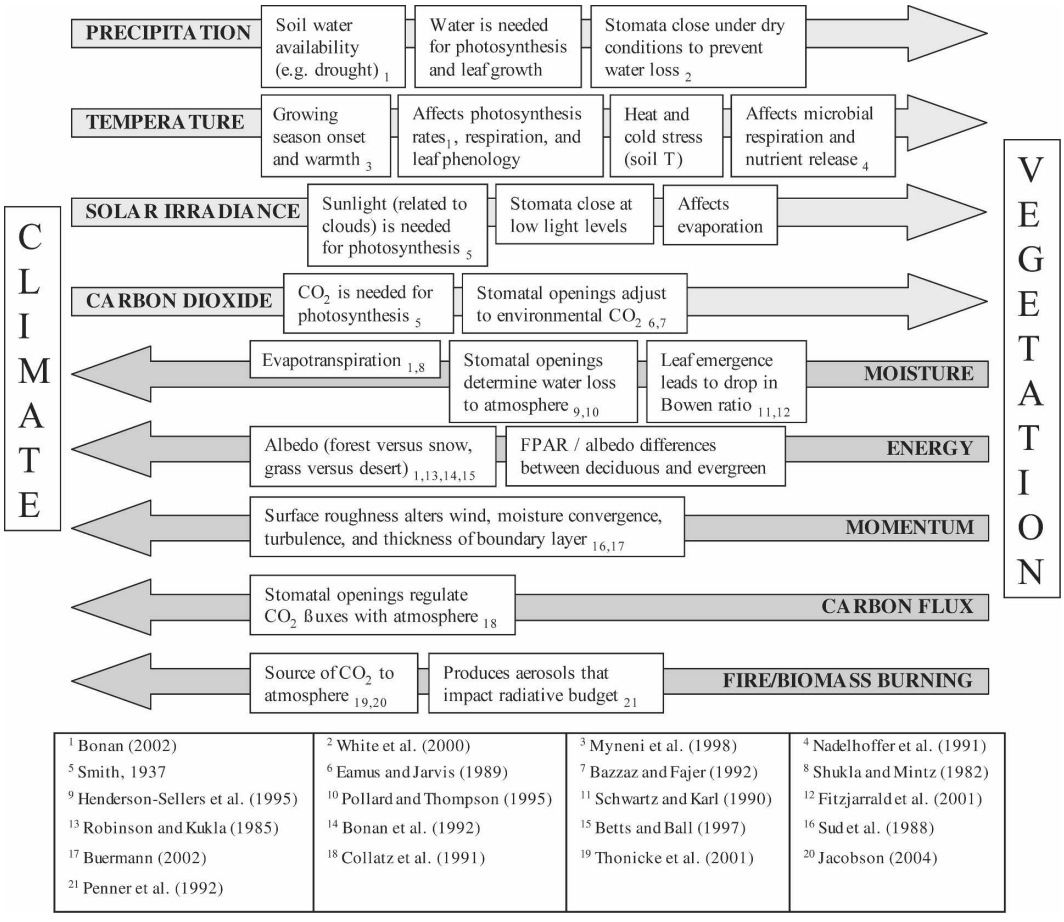

FIG. 1. Schematic of feedbacks between climate and vegetation on seasonal to interannual time scales.

Simulation of Interactive Systems–Integrated Biosphere Simulator (GENESIS–IBIS) led to cooling over the southern Sahara and Arabian deserts. Using the Community Climate System Model (CCSM2) with dynamic vegetation, Levis et al. (2004) concluded that soil feedbacks, linked to surface albedo changes, contributed to the northward advance of the North African monsoon during the mid-Holocene. Using the Fast Ocean Atmosphere Model–Lund Potsdam Jena (FOAM-LPJ) Gallimore et al. (2005) simulated a poleward expansion of boreal forest cover and an increase in midlatitude grasslands during the mid-Holocene, compared to simulated vegetation under modern orbital forcings. The expanded boreal forest, by masking snow cover, led to springtime warming through the albedo feedback. Notaro et al. (2005) simulated the impact of changes in CO_2 levels during the preindustrial to modern period, and likewise found a poleward shift of the boreal forest using FOAM-LPJ. Also, carbon dioxide fertilization produced a global greening trend and enhanced warming over Eurasia and North America.

Few studies have primarily applied observational data to determine the impact of vegetation feedbacks on the large-scale climate. Several studies determined that springtime leaf emergence initiates discontinuities in numerous meteorological variables (Schwartz and Karl 1990; Schwartz 1992, 1996; Fitzjarrald et al. 2001), while McPherson et al. (2004) showed that Oklahoma's winter wheat belt induces feedbacks on local temperature and moisture.

Using a satellite-based normalized difference vegetation index (NDVI) and gridded temperature data, Kaufmann et al. (2003) applied Granger causality statistics (Granger 1969) to quantify the effects of interannual variations in vegetation on temperature over North American and Eurasian forests. They found that increased NDVI over North America resulted in warming during winter and spring and cooling during summer and autumn. The impact on temperature was strongest during winter, when NDVI was negatively correlated with snow extent and weakly correlated with vegetation.

W. Wang et al. (2005, personal communication, here-

after W05) applied Granger causality to study intraseasonal interactions between NH vegetation and climate during the growing season. They identified significant causal relationships of vegetation on temperature and precipitation over the central North American grasslands, with enhanced vegetation leading to higher temperatures and reduced precipitation. This finding is not consistent with most modeling studies, which simulate an increase in precipitation resulting from an increase in vegetation.

Liu et al. (2006) estimated the magnitude of observed global vegetation feedbacks on temperature and precipitation. They used lead–lag correlations and a statistical feedback parameter (Frankignoul and Hasselmann 1977; Frankignoul et al. 1998) to relate the satellite-based fraction of photosynthetically active radiation (FPAR) to gridded temperature and precipitation data. They showed that, in the northern mid and high latitudes, vegetation variability is predominantly driven by temperature, while vegetation also exerts a strong positive feedback on temperature. They found that, while tropical and subtropical vegetation is mostly driven by precipitation, the influence of vegetation on precipitation is weak globally, with no evidence of a dominant positive vegetation–precipitation feedback.

Liu et al. (2006) used a statistical technique previously applied to ocean–atmosphere feedbacks to assess vegetation–climate feedbacks, thereby providing a global overview of vegetation impacts with limited attention given to underlying processes. This study applies the same statistical approach in a focused analysis of vegetation–climate feedbacks in the United States. In addition to presenting an overview of the mean and seasonality of vegetation in the United States and assessing the controls of vegetation growth, the magnitude of seasonal vegetation forcing on temperature and precipitation is quantified from observational data. The results can be applied to evaluate vegetation feedbacks in the United States as simulated by climate models.

The key difference between studies using a feedback parameter (present study; Liu et al. 2006) and those using Granger causality (Kaufmann et al. 2003; W05) is that the former is a feedback study that quantifies the instantaneous vegetation forcing on the atmosphere, while the latter is a predictability study of the causality between vegetation and the atmosphere at a later time. The present study and that of Liu et al. (2006) are the first to quantify the observed instantaneous forcing from vegetation. This instantaneous forcing (from feedback) will be greater than the lagged causality forcing (from predictability) with the difference representing the one-month FPAR autocorrelation (shown by Liu et al. 2006).

The data is outlined in section 2 and the methodology in section 3. Section 4 describes the mean, variance, and persistence of U.S. land cover and FPAR. Instantaneous and lead/lag correlations between FPAR and temperature/precipitation are the focus of section 5. Computed feedback parameters are presented in section 6. The conclusions are in section 7.

2. Data

Vegetation is assessed using the Pathfinder Version 3 Advanced Very High Resolution Radiometer (AVHRR) FPAR data (Myneni et al. 1997) on a $0.5° \times 0.5°$ grid. FPAR is the fraction of photosynthetically active radiation absorbed by the green parts of vegetation and represents a measure of vegetation activity. FPAR is derived from satellite-measured NDVI through a linear relationship (Myneni et al. 1997); FPAR can be directly computed from the model output, making it easier to use than NDVI to later assess model feedbacks. All data is obtained for 1982–2000. When computing correlations and feedback parameters, the data is interpolated to a $2.5° \times 2.5°$ grid, converted to monthly anomalies by removing the annual cycle, and linearly detrended.

Satellite-derived vegetation data contains certain known biases. Wintertime FPAR of high latitude forests is likely biased too low owing to the high albedo of snow cover and limited available sunlight for vegetation use or detection by remote sensing (Los et al. 2000; Buermann 2002; Tian et al. 2004). Pathfinder NDVI data is corrected for Rayleigh scattering (Gordon et al. 1988), ozone absorption, and instrument degradation, but not for aerosols or viewing geometry. Kaufmann et al. (2000) found that the data was not contaminated by trends associated with changes in solar zenith angle related to changing satellites or orbital decay. Huete (1988) and Kaufmann et al. (2000) determined that NDVI is sensitive to soil characteristics over partially vegetation regions. The vegetation feedback parameters in section 6 could include some signature of soil characteristics or snow cover. Model simulations can serve to further isolate actual vegetation feedbacks.

The sources of $2.5° \times 2.5°$ monthly climate data are the National Centers for Environmental Prediction–National Center for Atmospheric Research (NCEP–NCAR) reanalysis (Kalnay et al. 1996) for surface air temperature and Climate Prediction Center (CPC) Merged Analysis of Precipitation Dataset (Xie and Arkin 1997). FPAR, temperature, and precipitation data are used throughout sections 4–6. Mean tree cover fraction (total, deciduous, and evergreen) and grass, crop, and shrub cover fraction are retrieved from the Global

Continuous Fields of Vegetation Cover Dataset (DeFries et al. 1999, 2000). Crop cover fraction is obtained from Ramankutty and Foley's (1998) cropland dataset. The AVHRR-based biome distribution is retrieved from the Earth Resources Observation and Science (EROS) Data Center's Global Land Cover Classifications dataset (Loveland et al. 2001), which applies the International Geosphere–Biosphere Discover (IGBD) land cover legend (Loveland and Belward 1997). The forest cover fraction, crop cover fraction, and biome distribution datasets are applied in section 4.

3. Methods

Section 4b presents mean FPAR and computes the magnitude of FPAR's seasonal cycle and year-to-year variability using standard deviations. Unrotated (EOF) and rotated (REOF) empirical orthogonal functions are calculated using June–August (JJA) FPAR to investigate interannual variability. In section 4c, autocorrelation functions and decorrelation times are computed for FPAR, temperature, and precipitation anomalies. Decorrelation time represents memory or persistence and is computed by the following equation (von Storch and Zwiers 1999):

$$T_d = \frac{1 + \alpha_1}{1 - \alpha_1}, \tag{1}$$

where α_1 is the one-month autocorrelation.

Instantaneous and lead–lag correlations between FPAR and both temperature and precipitation are presented in sections 5a–c, using both data from all months and by season. The lead–lag correlations are extended in section 5d to regional analyses of Wisconsin and the central/northern Rockies, where significant correlations are identified with FPAR leading the atmosphere. Finally, feedback parameters are presented in section 6 as a measure of instantaneous forcing from FPAR.

The methodology of computing the feedback parameter for vegetation forcing on the atmosphere is outlined by Liu et al. (2006). It was initially proposed by Frankignoul and Hasselmann (1977) and later applied to study SST feedback on air–sea heat flux (Frankignoul et al. 1998; Frankignoul and Kestenare 2002) and the atmosphere's response to extratropical Atlantic (Czaja and Frankignoul 2002) and Pacific (Liu and Wu 2004; Lee and Liu 2005, manuscript submitted to *Climate Dyn.*) SSTs. As with SST, FPAR exhibits a longer memory than the atmosphere. In the present study, the impact of changes in monthly FPAR on temperature and precipitation are assessed over the United States. While feedback represents a two-way interaction, this study primarily focuses on the component of feedback with the vegetation forcing the atmosphere.

As shown by Liu et al. (2006), atmospheric variables such as temperature or precipitation can be divided into two components:

$$A(t + dt_a) = \lambda_A V(t) + N(t + dt_a). \tag{2}$$

Here $A(t)$ is the atmospheric variable at time t, $V(t)$ is FPAR at time t, λ_A is the feedback parameter, dt_a is the atmospheric response time (about one week), and $N(t)$ is the climate noise generated internally by atmospheric processes that are independent of FPAR variability. The atmospheric variable is determined by $\lambda_A V(t)$, which is its feedback response to changes in FPAR, and $N(t + dt_a)$, which is atmospheric noise. As derived by Liu et al. (2006) and Frankignoul et al. (1998), the feedback parameter can be determined as

$$\lambda_A = \frac{\text{covar}[A(t), V(t - \tau)]}{\text{covar}[V(t), V(t - \tau)]}, \tag{3}$$

where τ is the time lag, which is longer than the persistence time of atmospheric internal variability. The feedback parameter is estimated as the ratio of the lagged covariance (covar) between A and V to the lagged covariance of V. Following Frankignoul et al. (1998), the feedback parameter is computed as the weighted average from the first three lags (weights of 1.0, 0.5, and 0.25 for lags of 1, 2, and 3 months, respectively).

The feedback parameter quantifies the instantaneous feedback response of the atmosphere to changes in FPAR based on monthly data. For surface air temperature, λ_T is given in units of °C $(0.1\ \text{FPAR})^{-1}$, representing the change in observed temperature due to an increase in monthly FPAR by 0.1. For precipitation, λ_P is given in units of cm month^{-1} $(0.1\ \text{FPAR})^{-1}$. Positive values of λ indicate a positive forcing of FPAR on the atmospheric variable. To estimate the statistical significance of the feedback parameters, a Monte Carlo bootstrap approach is applied in which 1000 individual λ are computed at each grid point from shuffled series (Czaja and Frankignoul 2002). The significance is determined by the percentage of these λ that are smaller in magnitude than the actual computed feedback parameter for that grid cell.

Kaufmann et al. (2003) noted that conventional lagged correlations are insufficient to determine causality within the fully coupled earth system owing to issues of persistence. Kaufmann et al. (2003) and W05 applied Granger causality statistics in order to better isolate cause and effect in the coupled climate–vegetation system. Granger causality incorporates lagged cross-correlations and autocorrelations, thereby attempting

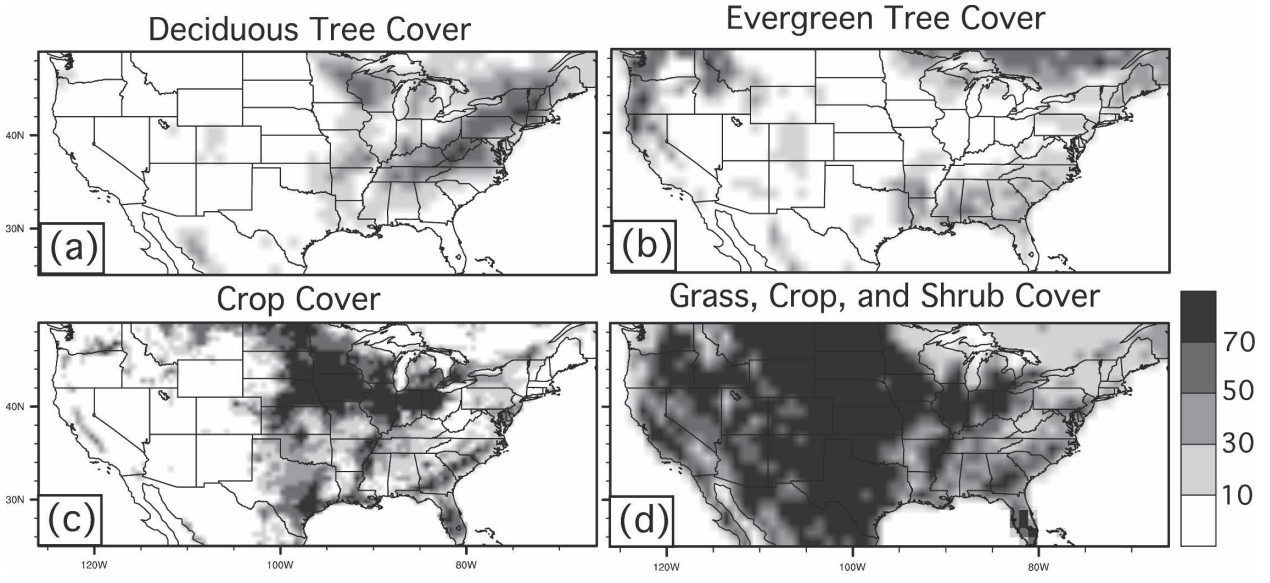

FIG. 2. Percent coverage of (a) deciduous trees, (b) evergreen trees, (c) crops, and (d) grasses/crops/shrubs. The data source for (a), (b), and (d) is the Global Continuous Fields of Vegetation Cover Dataset (DeFries et al. 1999, 2000) and for (c) Ramankutty and Foley's (1998) cropland dataset.

to extract causality without false signals from persistence. However, this methodology is new to climate studies (Kaufmann and Stern 1997) and has received some criticism regarding the interpretation of its results for a multivariate system (Triacca 2001). The feedback parameter in the present study also considers both lagged cross-correlations and autocorrelations, providing a higher order statistical analysis to supplement the basic correlations in section 5. Nonetheless, without using a climate model, it is difficult using pure statistical methods to extract causality within a fully coupled earth system due to numerous feedbacks and persistence. The present study offers a statistical approach to quantify observed vegetation forcing on the atmosphere but does not attempt to explain all the mechanisms involved.

4. U.S. land cover and FPAR

a. Land cover dataset description

Figure 2 presents the percent coverage of deciduous trees, evergreen trees, grass/herb/shrubs, and crops across the United States, while the IGBD biome distribution is shown in Fig. 3. Total tree cover is limited to 35% of the United States. Evergreen forests cover 21% of the country, including the coastal plain evergreens of the Southeast, Pacific Coast evergreens of the Northwest, and boreal forest extending into Minnesota, Michigan, and New England. Deciduous forests extend across 14% of the United States, predominantly in the Mid-Atlantic, Northeast, and Midwest states.

The majority of the country, 52%, is covered by grassland, shrubland, and cropland. The mountainous land between 120° and 105°W is predominantly shrubland and grassland. The Great Plains prairie, which today is largely cropland and pastureland, lies from the eastern slope of the Rockies to about 94°W, the western edge of the eastern U.S. mixed forest. The Corn Belt, with mostly maize and soybean, stretches from the Dakotas to Ohio. Substantial amounts of spring (winter) wheat are grown in the Dakotas and Montana (Kansas, Colorado, Oklahoma, and Texas).

b. Mean, seasonality, and interannual variability of FPAR and climate variables

Mean FPAR is greatest over the deciduous and evergreen forests of the East and the Pacific Northwest evergreen forests (Fig. 4). While evergreen forests maintain the highest wintertime FPAR values (0.5–0.7), the thick leaf cover of deciduous forests in the eastern United States leads to higher summertime FPAR values (0.7–0.9). Year-round warm, wet conditions in the Southeast and wet, relatively mild winter conditions in the Pacific Northwest help maintain evergreen forests. A strong southerly low-level jet advects warm, moist Gulf air across the central U.S. prairie during summer. The eastern edge of this prairie represents a climatic boundary where precipitation exceeds evaporation to the east and vice versa to the west. Across the north United States, limited growing degree-days and sun-

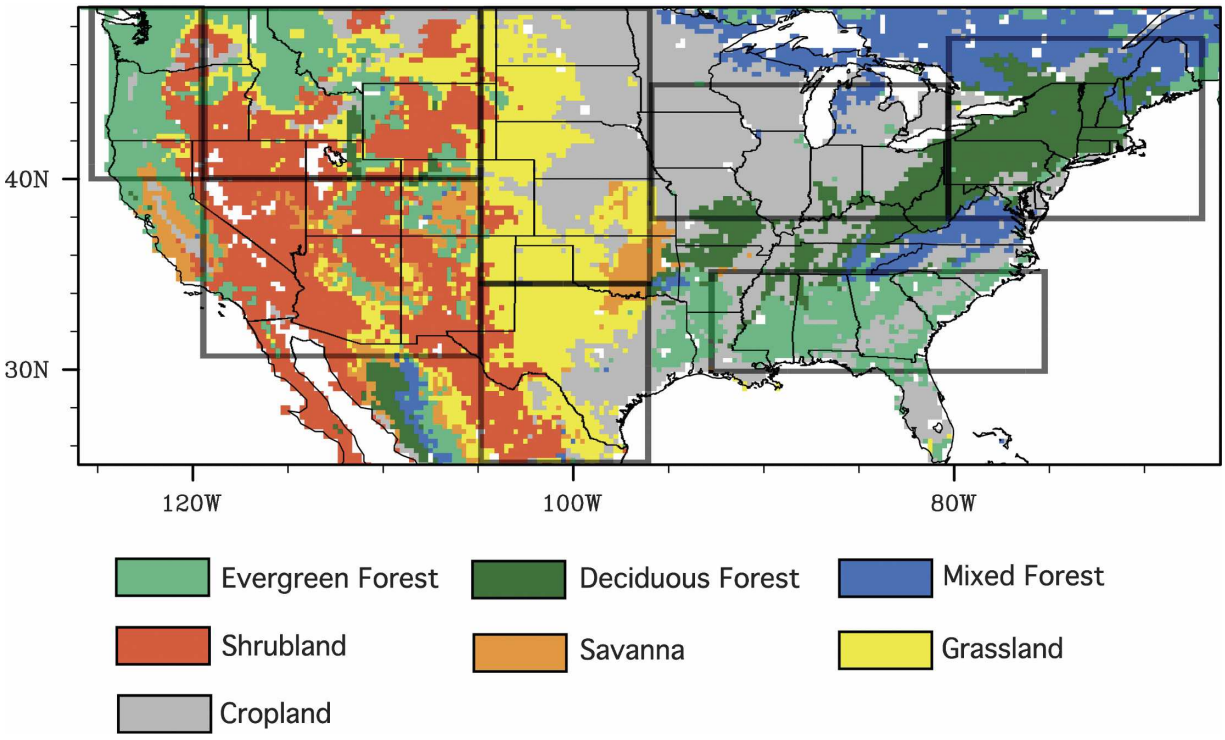

FIG. 3. Biome distribution from EROS Data Center's Global Land Cover Classifications dataset (Loveland et al. 2001), which was derived from AVHRR data for 1992–93 and applies the IGBD land cover legend (Loveland and Belward 1997). Classifications are merged into seven categories for simplification. Boxes indicate the eight regions in Table 1.

light contribute to low wintertime FPAR values (except the Pacific Northwest). The southern extent of the North American boreal forest follows the mean winter position of the Arctic front (Bryson 1966). Poleward of 36°N, FPAR peaks during summer at most locations within the United States. In the Southeast and the Southwest monsoon region, FPAR typically peaks in autumn, although its seasonal cycle is quite weak. Isolated areas of the southern prairie and southern California achieve maximum FPAR in spring.

FPAR, temperature, and precipitation are averaged over each season and the interannual variability for each season is shown in Fig. 5. Two centers of high interannual variance in FPAR are identified over the northern (Dakotas/Montana) and southern (Texas) Great Plains, connected by a saddle of high variance across the plains, while interannual variability is minimal to the east of 95°W and across the Southwest. The interannual standard deviation of FPAR reaches 0.06 at both centers in summer, although the northern center is more distinct in winter and corresponds to the location of largest temperature variance (Fig. 5). Grasslands and shrublands support substantial year-to-year summertime FPAR variance, while agricultural regions of the eastern Dakotas/Minnesota and eastern Texas exhibit less variance. Previous studies have noted large interannual variability in aboveground net primary productivity (Knapp and Smith 2001) and fractional vegetation cover (Myneni et al. 1998; Zeng et al. 2003) of grasslands. The Pacific Coast evergreen forests exhibit large year-to-year FPAR variance, mostly between winters, due to large precipitation variance.

Across the northern United States, FPAR exhibits a strong seasonal cycle (Fig. 6b) associated with a distinct temperature seasonal cycle. The standard deviation of the climatological monthly mean FPAR, representing its seasonal cycle, exceeds 0.3 over North Dakota and Minnesota where temperature variance is particularly large in winter and spring (Fig. 6b). The standard deviation of monthly FPAR anomalies (after removing the seasonal cycle) is mostly less than 0.1 and peaks in the northern prairie and the Northeast, due to temperature variance and in the Northwest and southern prairie, due to precipitation variance (Fig. 6c). It is substantial in comparison to the amplitude of FPAR's seasonal cycle over the southern prairie, Southeast coastal plain evergreens, and Pacific Coast evergreens (Fig. 6d). In these coastal areas, there is large year-to-year variance

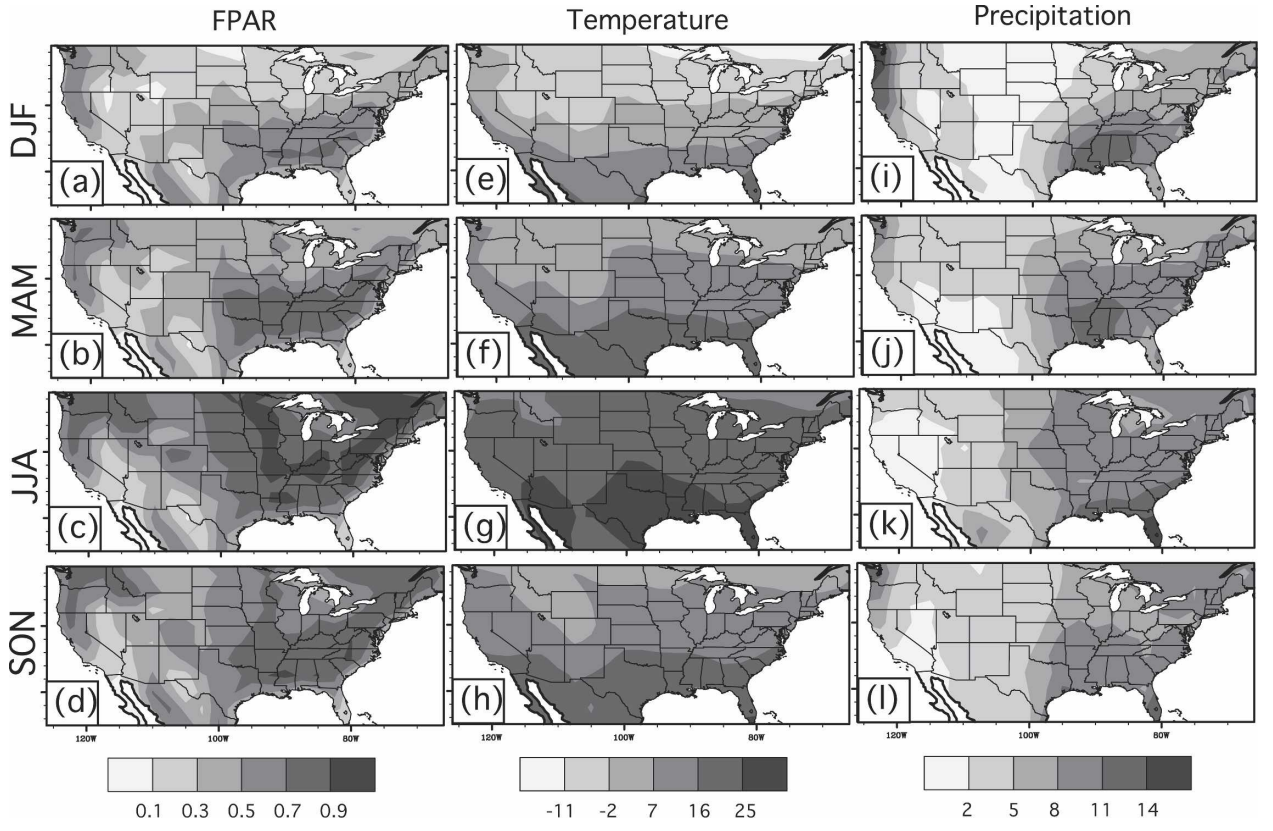

FIG. 4. Mean (a)–(d) FPAR (Myneni et al. 1997), (e)–(h) surface air temperature (°C) (Kalnay et al. 1996), and (i)–(l) precipitation (cm month^{-1}) (Xie and Arkin 1997) for the four seasons.

associated with ENSO, as well as a weak seasonal cycle; in the Great Plains, year-to-year monthly variability of FPAR is also high due to large variance in temperature and precipitation. Consequently, in these regions the yearly variability of monthly anomalies is more comparable with the amplitude of the seasonal cycle than is the case over much of the country.

The interannual variance of FPAR is investigated with unrotated and rotated EOFs (Fig. 7). Based on REOF-1 and EOF-1 for JJA, the centers of enhanced FPAR anomaly variance over the northern prairie and southern prairie/Mexico act as a dipole. The dipole pattern of REOF-1 comprises 30% of the variance in FPAR anomalies across the United States. This north–south dipole signature in FPAR is distinct in the El Niño summer of 1987 and La Niña summer of 1998. A somewhat similar north–south pattern is observed in REOF-1 and -2 for JJA surface air temperature. W05 identified the area of this northern dipole center as a region of significant vegetation feedbacks. The large FPAR variance over the prairie (Figs. 5 and 7) reflects the high biomass turnover rate of grasslands compared to forests, which allows for rapid response to interannual atmospheric variability.

c. *Persistence*

Spatial maps of the FPAR decorrelation time and autocorrelation are produced to investigate its memory, or persistence (not shown). The decorrelation time of monthly FPAR anomalies is typically two to four months across the prairie and Rocky Mountain shrublands and grasslands, but is mostly less than two months over the Corn Belt and eastern deciduous forest. One-month autocorrelations exceed 0.4 across the prairie and the West, suggesting a strong short-term memory for grasslands and shrublands. However, six-month autocorrelations are largest over the Southeast coastal plain evergreens. Based on the statistical significance of autocorrelations at different lags, the average U.S. FPAR memory is four months.

The United States is divided into eight regions based on biome classifications and geography, and the memory (based on autocorrelation) of FPAR, temperature, and precipitation is determined from area averages for each region (Table 1). One-month autocorrelations are low for temperature (0.10–0.30) and precipitation (0.04–0.20), although regions of the West exhibit memories of 1–2 months. Since the true atmospheric

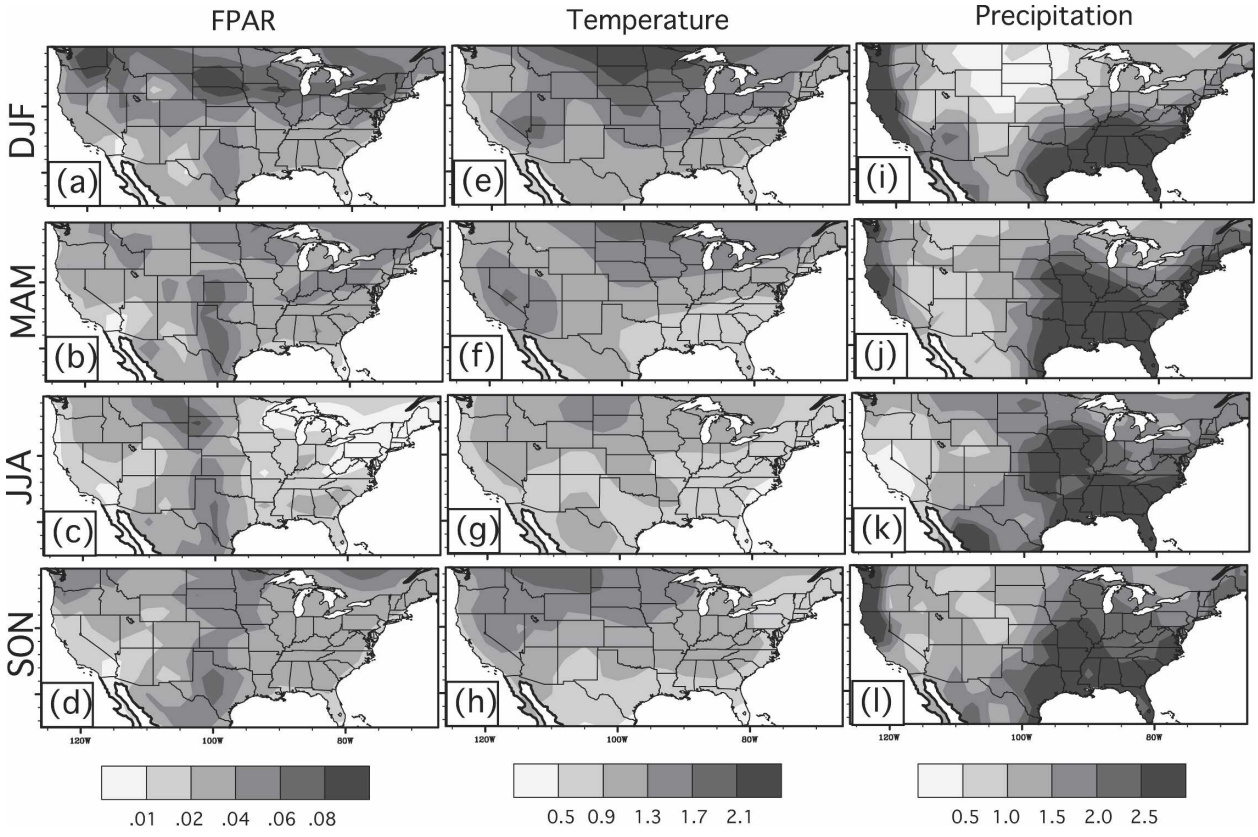

FIG. 5. As in Fig. 4 except for the standard deviation.

memory is less than one week, these longer memories perhaps reflect contributions from soil moisture, vegetation, and SSTs.

FPAR exhibits a longer memory than the atmosphere, with statistically significant one-month autocorrelations ranging from 0.24 in the Corn Belt to 0.51 in the southern prairie. One-month autocorrelations are weakest across the eastern forests and Corn Belt and strongest across the prairie and Rockies, where mostly grass and shrubs grow. The low one-month autocorrelations of eastern biomes reflect ample moisture supply, limited sensitivity to climatic variability, and low FPAR variability. FPAR has a significant memory of at least four months in the Southeast, southern prairie, and southern Rockies, suggesting a longer memory across the southern states. The enhanced sensitivity of northern biomes to instantaneous temperature variability supports their limited memory. The substantial FPAR memory across the prairie is surprising, but could partly reflect the ongoing influence of precipitation across several preceding months, the substantial memory of the groundwater system, and the resilient nature of grass (Risser 1985). Likewise, other studies have found substantial soil moisture memory over the western half of the United States (Maurer et al. 2002; Wu and Dickinson 2004).

The Southeast coastal plain evergreens have a relatively weak, yet significant, one-month autocorrelation of 0.28, but exhibit significant memory beyond ten months. Within a forest, FPAR is comprised of both a relatively fast-changing leaf coverage and slow-changing total vegetation coverage; this partly explains the sudden drop in autocorrelation after one month and the continued weakly significant autocorrelations over many monthly lags. The opposite is noted for the Pacific Coast evergreens, where the FPAR one-month autocorrelation reaches 0.43 but significant memory is limited to one month. The FPAR autocorrelation curve for the Southeast evergreens shows a relative peak at lags of four to six months (Fig. 8), implying enhanced cross-seasonal memory.

The memory computed in this section can potentially reflect the influence of local forcings, such as soil moisture, or remote forcings, such as SST and teleconnections. Walsh et al. (1985) showed that SST, soil moisture, and sea ice have a substantial memory compared to atmospheric circulation. These slow-changing variables, in addition to vegetation, largely explain the ap-

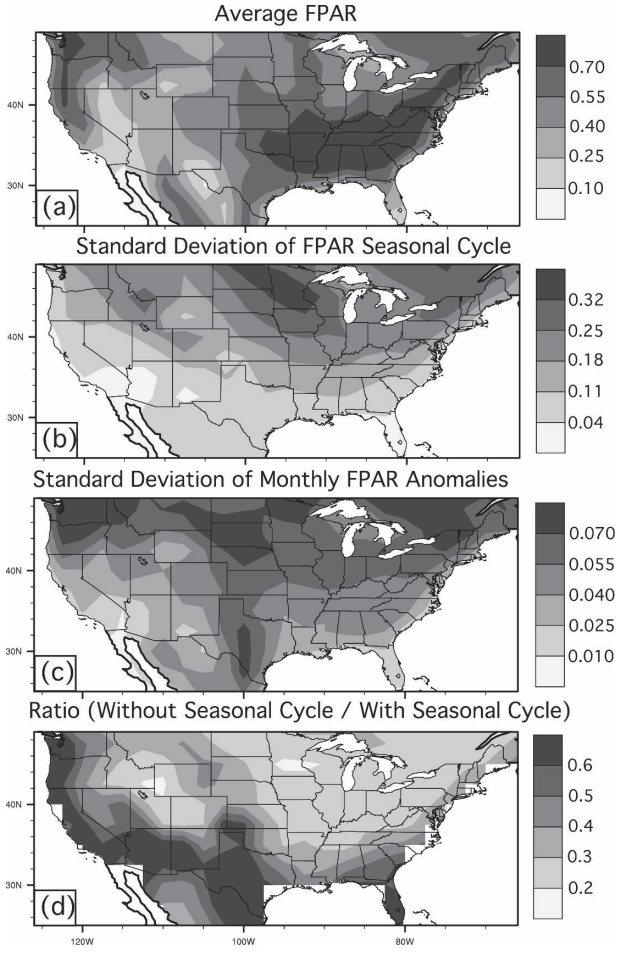

FIG. 6. (a) Mean annual FPAR, (b) standard deviation of the FPAR's seasonal cycle, and (c) standard deviation of monthly FPAR anomalies (seasonal cycle removed); (b) and (c) compare the strength of FPAR seasonal cycle to the variability of its monthly anomalies. The ratio of the standard deviations of monthly FPAR anomalies and FPAR seasonal cycle is shown in (d).

parent memory of temperature and precipitation beyond a few days. Since such variables influence vegetation, it is likely that they maintain a signature in the FPAR data that is difficult to separate within observational data.

5. Relationship between FPAR and atmospheric variables

a. Instantaneous correlations

Previous studies have correlated global NDVI to both temperature and precipitation. Vegetation changes in northern temperate climates were linked to temperature by Los et al. (2001) and Ichii et al. (2002) and to both temperature and precipitation by Schultz and Halpert (1993). Here, the approach is extended by calculating instantaneous (same month) correlations between monthly FPAR and both temperature and precipitation anomalies in the United States for each season (Fig. 9). While these instantaneous correlations primarily reflect the response of vegetation to atmospheric conditions, a portion of the instantaneous relationships can be attributed to vegetation forcing the atmosphere. On time scales of less than one month, the large internal atmospheric variability exceeds the slow variance in FPAR, supporting the atmosphere as an important "instantaneous" driver of vegetation.

The instantaneous relationship between FPAR and temperature is stronger than for precipitation. Monthly FPAR anomalies are significantly correlated with temperature throughout most of the country, except in the far South where there is sufficient warmth and limited temperature variability. In warm regions, temperature exceeds the minimum needed for vegetation growth and therefore does not substantially impact the vegetation seasonal cycle (Schultz and Halpert 1993). Across all months, the correlation between monthly FPAR anomalies and temperature anomalies exceeds 0.4 in the croplands of the upper Midwest (Fig. 9e).

The strongest positive correlation between FPAR and temperature is found over the northern half of the United States during December–February (DJF) and March–May (MAM) (Figs. 9a,b). While it is unclear if the DJF correlation is mostly a snow signature, the positive MAM correlation likely reflects the sensitivity of vegetation phenology to temperature. Temperature regulation of phenology is an important process except during peak growing season. It is particularly critical during spring, affecting spring budburst and leaf senescence, and across the northern regions (snow masking and melting are also important). The positive correlation between FPAR and temperature during JJA and September–November (SON) in the northern Rockies indicates reduced vegetation activity during cooler and/or shorter growing seasons (Figs. 9c,d). Vegetation in cold regions is typically limited by temperature (Schultz and Halpert 1993). The positive instantaneous correlations between growing season FPAR and temperature anomalies across the North and West agree with W05.

Monthly FPAR anomalies are positively correlated with instantaneous precipitation anomalies in the southern prairie but only weakly significant (Fig. 9j). FPAR typically responds to precipitation with a one-month lag (section 5b). The statistically significant, positive instantaneous correlation is strongest over Texas as the low-level jet (LLJ) supplies Gulf of Mexico moisture to the southern prairie. This suggests that gulf transport is variable and affects the southern

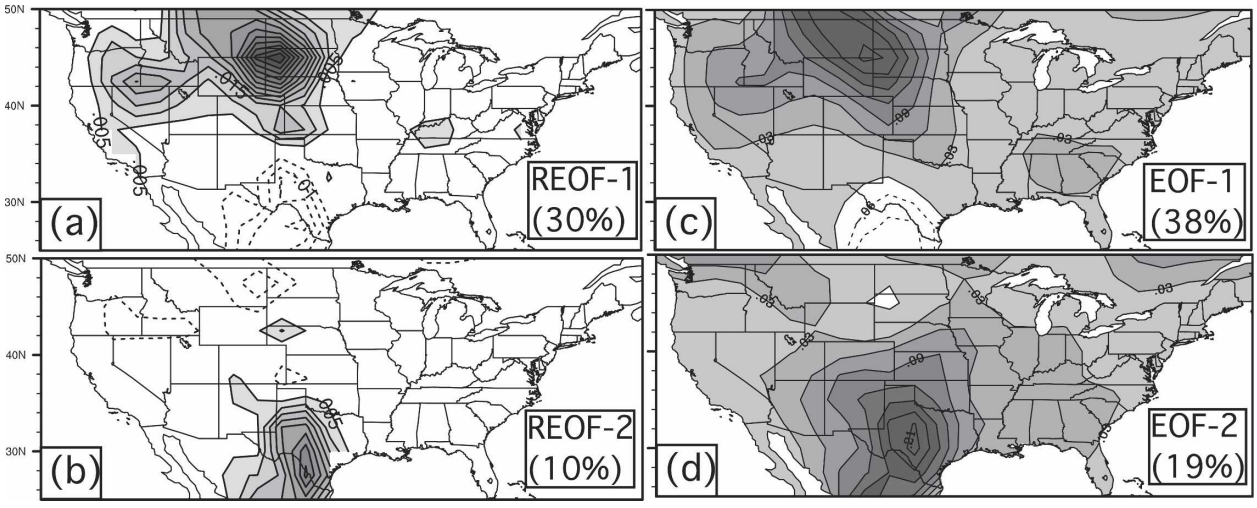

FIG. 7. REOF and EOF patterns for JJA FPAR anomalies: (a) REOF-1, (b) REOF-2, (c) EOF-1, and (d) EOF-2. The percent explained variances are 30%, 10%, 38%, and 19%, respectively. Shading indicates positive values.

prairie ecosystems. Neither temperature nor precipitation significantly force FPAR in the Southeast due to year-round warm, wet conditions, while partly reflecting limited FPAR variance (Fig. 6). East of the prairie, precipitation typically exceeds evaporation and is more than sufficient to maintain higher FPAR, thereby explaining an absence of positive correlations between FPAR and precipitation. Also, forests are efficiently buffered against climatic fluctuations due to their deep roots and access to deep-soil moisture (Wang et al. 2003). Across the West, instantaneous correlations suggest that FPAR is negatively correlated with precipitation (Fig. 9j) but positively correlated with temperature (Fig. 9e) (Schultz and Halpert 1993), particularly early in the growing season (MAM) when temperature largely determines plant growth. There is an intrinsic negative correlation between temperature and precipitation in the West that is not easily separated in observations. Vegetation in the Northwest United States is temperature driven, and an increase in precipitation and clouds can reduce photosynthesis (Schultz and Halpert 1993).

b. Correlations with atmosphere leading

While temperature has a more instantaneous relationship with FPAR (W05), precipitation generally exhibits its strongest forcing when leading by one month. Figure 10 shows the correlations between temperature/precipitation and FPAR, with the atmospheric variables leading by one month. Across all months, temperature imposes a weak positive forcing on FPAR when leading by one month for most of the country (Fig. 10e). This positive forcing is greatest during MAM in the Midwest (Fig. 10b), where a rise in temperature accelerates the onset of the growing season. The MAM correlations for temperature are typically positive

TABLE 1. Estimations of observed FPAR, surface air temperature, and precipitation persistence in eight regions of the United States. For each variable, the maximum lag, in months, that achieves statistical significance (90%) in an autocorrelation curve ("FPAR memory") (significant at that lag and all shorter lags) and the one-month autocorrelation value (FPAR AC) are provided. One-month autocorrelations in bold have achieved 90% significance. The map shows the location of the eight regions.

	FPAR		Temperature		Precipitation	
Region	Memory	AC	Memory	AC	Memory	AC
Northeast (NE)	1	**0.25**	0	0.10	0	0.04
Southeast (SE)	10+	**0.28**	1	**0.19**	0	0.08
Corn Belt (CB)	1	**0.24**	1	**0.15**	0	0.08
N. Prairie (NP)	2	**0.41**	1	**0.23**	0	0.05
S. Prairie (SP)	4	**0.51**	1	**0.19**	1	**0.12**
N. Rockies (NR)	2	**0.41**	2	**0.22**	1	**0.17**
S. Rockies (SR)	4	**0.45**	2	**0.30**	2	**0.20**
Northwest (NW)	1	**0.43**	2	**0.22**	1	**0.18**

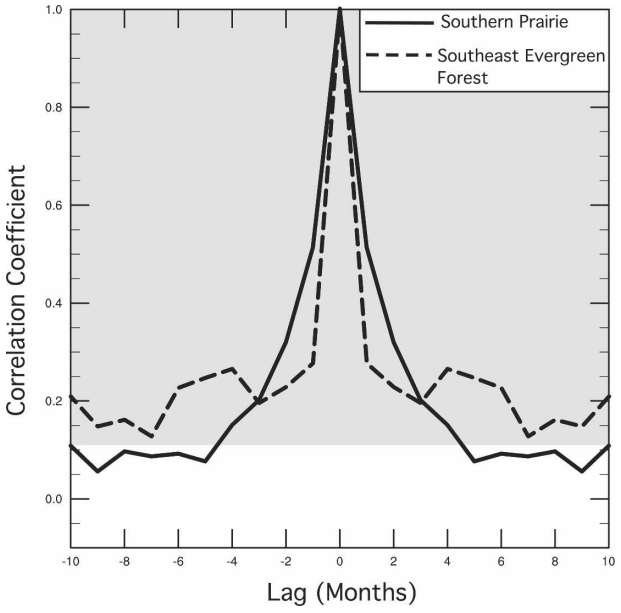

FIG. 8. Temporal autocorrelation of monthly FPAR anomalies for the southern prairie (solid) and Southeast evergreen forests (dash). Correlation coefficients are shown at different time lags up to 10 months. Shading indicates 90% significance level. The autocorrelation is a measure of memory or persistence.

(negative) over the coldest (warmest) regions. The higher correlations in MAM than in SON agree with W05, suggesting that temperature imposes a stronger control on vegetation earlier rather than later in the growing season. During JJA (Fig. 10c), temperature leading by one month is negatively correlated with FPAR in the prairie (significant in the southern prairie); precipitation is the primary forcing on FPAR when leading by one month, and temperature and precipitation are inversely related in the prairie. This inverse relationship is strongest over the western prairie. A statistically significant positive correlation is found between precipitation and the following month's FPAR across the southern prairie in every season and much of the prairie during JJA, during which precipitation provides the soil moisture needed for plant growth to this moisture-limited region (Figs. 10f–j). The advection of Gulf moisture into the midcontinent is an important control of FPAR. Both instantaneous and one-month lead correlations reveal the strongest temperature forcing on FPAR in MAM (e.g., Midwest) and strongest precipitation forcing during the growing season in JJA (e.g., southern prairie).

While FPAR is most related to instantaneous temperature and the previous month's precipitation, anomalies of either variable over previous seasons can contribute toward summertime FPAR anomalies. FPAR anomalies for JJA are correlated against temperature and precipitation anomalies during time periods of varying length up to and through summer (Fig. 11). Much of the East/Southeast and West shows no significant relationship between FPAR and temperature due to limited temperature variability, sufficient warmth, and the influence of relatively warm winter and spring SSTs. Across the northern prairie and Corn Belt, the highest correlation is achieved between JJA FPAR anomalies and March–August temperature anomalies with a warm spring and summer supporting above-normal summertime FPAR. The North American boreal forest is the only vast forest region with significant FPAR correlation to spring–summer mean temperature anomalies. Summertime FPAR of most forests in the United States is either independent of temperature or best correlated with summertime temperature only, while FPAR in grasslands/shrublands is best correlated with temperature anomalies averaged through late winter to summer.

Across the prairie and portions of the West, JJA FPAR exhibits the strongest correlation with precipitation anomalies averaged over the summer and several preceding months; in these relatively drier regions, positive precipitation anomalies are needed over an extended period to supply sufficient soil moisture for sustained, widespread plant growth. The hydrological reservoirs in plants and soil serve as critical buffers, making plants relatively insensitive to brief wet and dry periods but vulnerable to the cumulative effect of multimonth droughts. Grass exhibits several adaptive strategies, including stomata closure and leaf curling during drought (Risser 1985). Wang et al. (2001, 2003) and Adegoke (2000) likewise found that vegetation growth is most influenced by precipitation during a preceding period of multiple months for Kansas and the Midwest, respectively. The eastern forests show little relationship with precipitation owing to sufficient soil moisture from ample precipitation.

c. Correlations with FPAR leading

Correlations with FPAR leading temperature and precipitation by one month hint at observed vegetation impacts on climate (Fig. 12). Across all months (Fig. 12e), FPAR is significantly positively correlated ($p < 0.05$) to the next month's temperature across the northern United States. Globally, positive correlations extend across the boreal forests (Liu et al. 2006), with the positive correlations over northern United States representing the southern edge of the Canadian boreal forest correlation maximum. Vegetation cover at the mid and high latitudes masks the high reflectivity of snow, leading to higher temperatures than if the vegetation was absent (Fig. 1) (Bonan et al. 1992; Betts and Ball

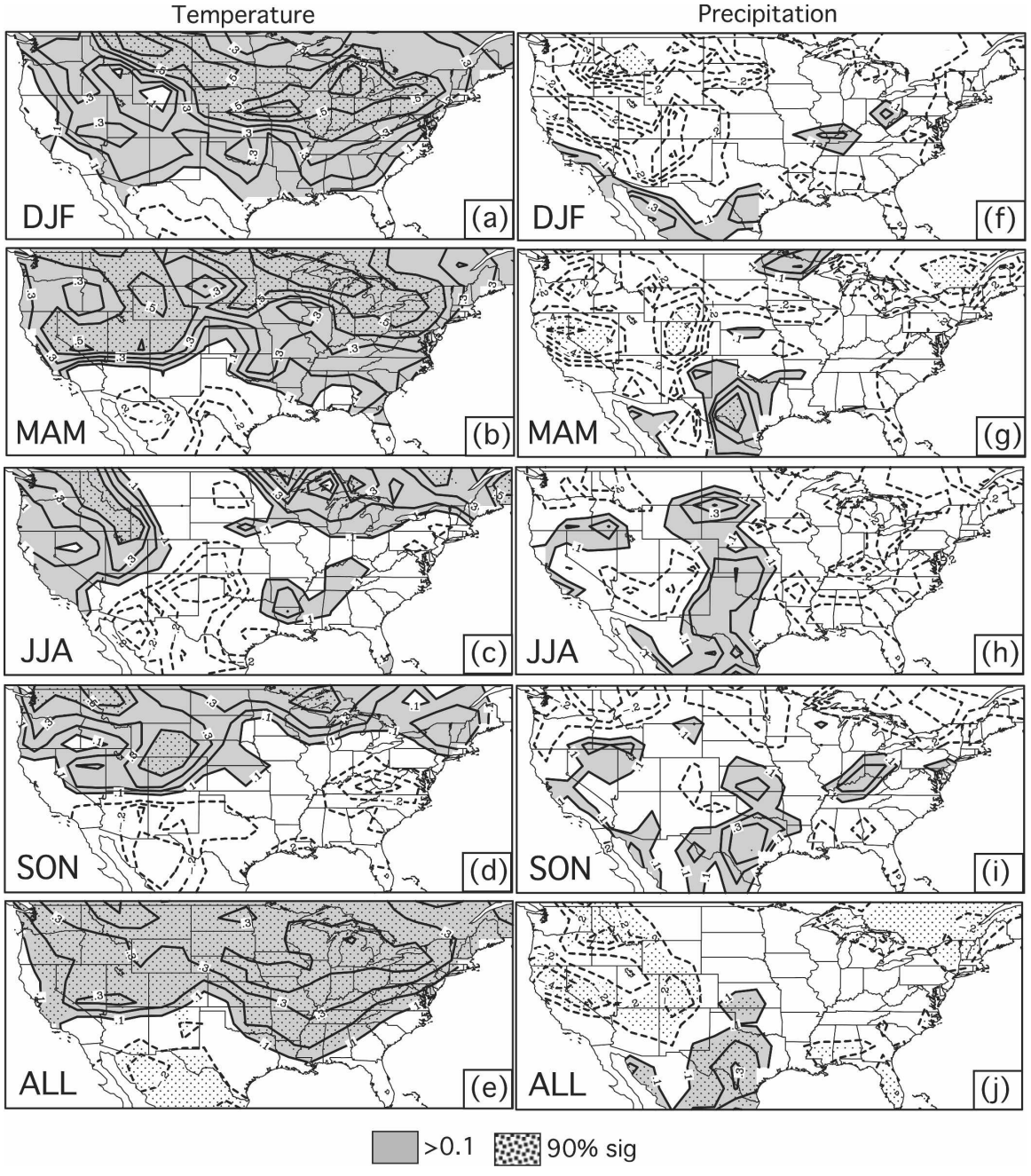

FIG. 9. Instantaneous correlations between monthly FPAR anomalies and monthly anomalies of (a)–(e) surface air temperature and (f)–(j) precipitation. Correlation coefficients are shown for (a), (f) DJF; (b), (g) MAM; (c), (h) JJA; (d), (i) SON; and (e), (j) all months. For example, for each grid point the JJA correlation coefficients for temperature are computed as the average of three correlation coefficients: June temperature vs June FPAR, July temperature vs July FPAR, and August temperature vs August FPAR.

1997). The albedo of snow cover reaches 35%–90%, compared to 10%–20% for most vegetation (Hartmann 1994). Even in the absence of snow cover, higher FPAR leads to greater energy absorption by lowering albedo, and thus higher temperatures; this largely explains the positive correlations in Fig. 12 over the Midwest in MAM and the Rockies in JJA.

The positive correlation with FPAR leading temperature is weakly significant ($p < 0.10$) over the upper Midwest in MAM (Fig. 12b) and the northern Rockies in JJA (Fig. 12c). The positive FPAR forcing on temperature in MAM is greatest over the croplands (and forests) of the upper Midwest and larger than the nearby Canadian boreal forest and the eastern decidu-

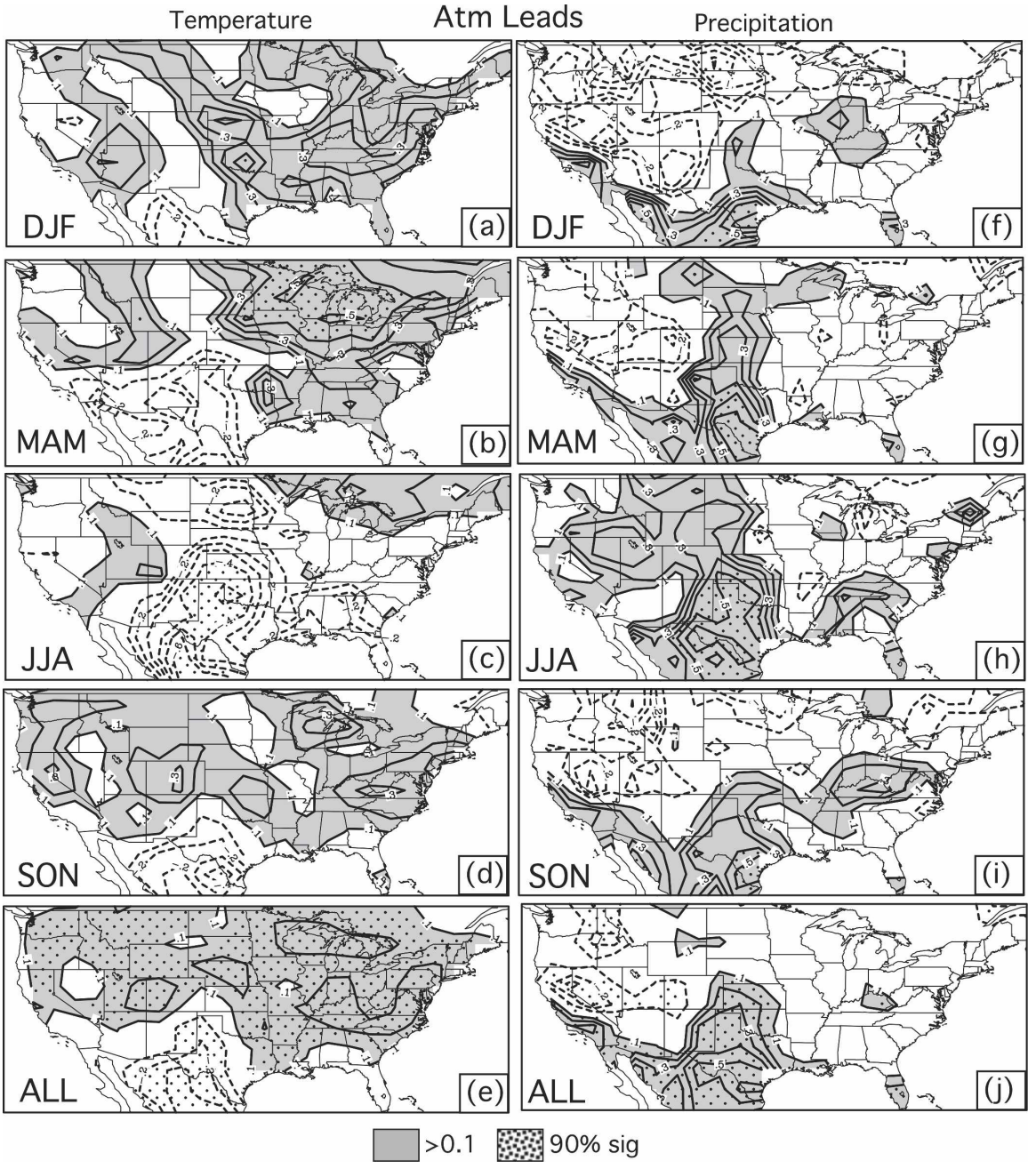

FIG. 10. As in Fig. 9 except that the atmospheric variables lead by one month. For example, for each grid point, the JJA correlation coefficients for temperature are computed as the average of three correlation coefficients: May temperature vs June FPAR, June temperature vs July FPAR, and July temperature vs August FPAR. These correlations suggest atmospheric forcing on vegetation.

ous forests. An increase in FPAR over the Corn Belt can mask springtime snow cover, producing substantial positive feedback on temperature. Likewise, partial correlations, which remove the effects of temperature persistence, reveal significant positive forcing ($p < 0.10$) of April FPAR on May temperature in the upper Midwest and Great Lakes Basin and of July–August FPAR on August–September temperature over the northern Rockies.

Correlations with FPAR leading precipitation (Figs. 12f–j) fail to show substantial areas with FPAR significantly impacting precipitation. These findings suggest the importance of vegetation albedo feedback while hinting at a weaker than expected moisture feedback. It

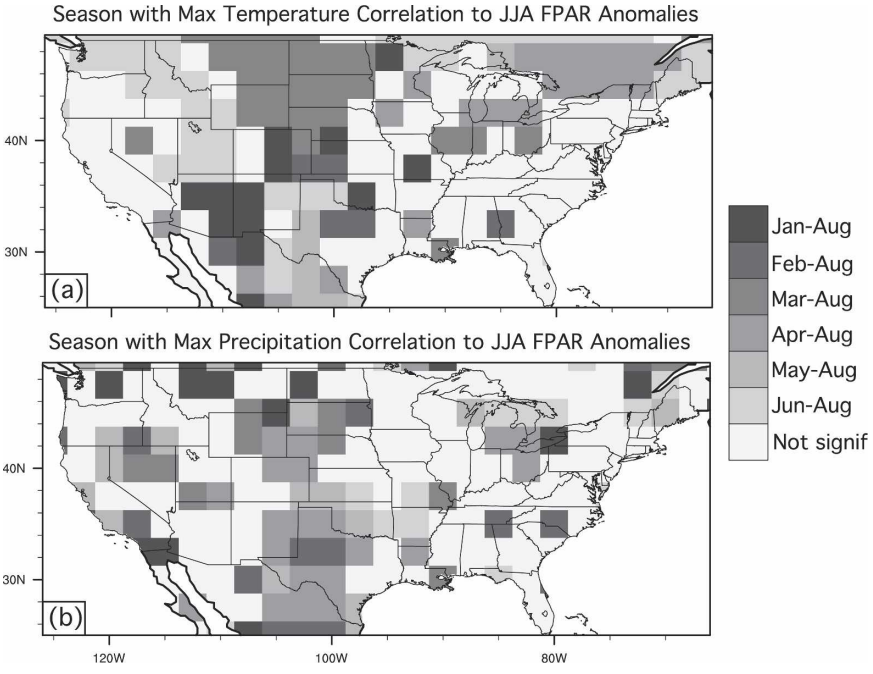

FIG. 11. (a) Period with maximum correlation between JJA FPAR anomalies and temperature anomalies. Shading represents periods ranging from June–August to January–August, with nonsignificant correlations left in white. (b) As in (a) except correlating JJA FPAR anomalies with precipitation anomalies of different periods.

is possible that the hydrological impact of vegetation has been largely overstated in modeling studies or that limited data availability is partly responsible for failure to achieve a statistically significant correlation between FPAR anomalies and subsequent month's precipitation. Advection by the atmospheric circulation can transport the transpired moisture downstream, where it precipitates, resulting in a nonlocal feedback that would be missed by these correlations. Brovkin (2002) suggested that vegetation imposes a substantial local forcing on temperature by modifying the local radiative budget, while its impact on atmospheric moisture is potentially remote due to transport. While the forcing of FPAR on precipitation one month later appears weak, it is also possible that this forcing is more substantial on a different time scale (e.g., instantaneous or at a longer lag).

d. Regional analyses

Regional interactions between the atmosphere and vegetation are investigated over Wisconsin, the central/northern Rockies, and the two FPAR dipole centers. The first two regions are selected based on relatively strong FPAR-leading temperature correlations (Fig. 12) and mostly uniform biome classifications, while the dipole centers are investigated to determine the source of their FPAR variability and possible vegetation feedbacks.

Wisconsin is characterized mainly by croplands, with some mixed forests in the northern part of the state. The instantaneous correlation between Wisconsin's monthly FPAR and temperature anomalies is largest, while correlations with either FPAR or temperature leading by one month are also significant ($p < 0.10$) (Fig. 13). There is evidence of two-way forcing between the atmosphere and vegetation. The instantaneous correlation between FPAR and temperature anomalies is significant during spring and autumn ($p < 0.05$) but minimal during summer, suggesting that high temperatures in the transition seasons encourage vegetation growth. Temperature forcing of FPAR is greatest in spring, with springtime temperatures significantly correlated ($p < 0.05$) with spring–summer FPAR anomalies. The onset of the growing season depends on springtime temperatures and the accumulation of growing season warmth. Positive significant ($p < 0.10$) forcing of vegetation on temperature is noted in spring and autumn, particularly between April FPAR anomalies and May temperature anomalies (also Fig. 12b). There is evidence of a positive forcing of the preceding July–October FPAR anomalies on October temperature, suggesting a possible crop feedback on surface albedo.

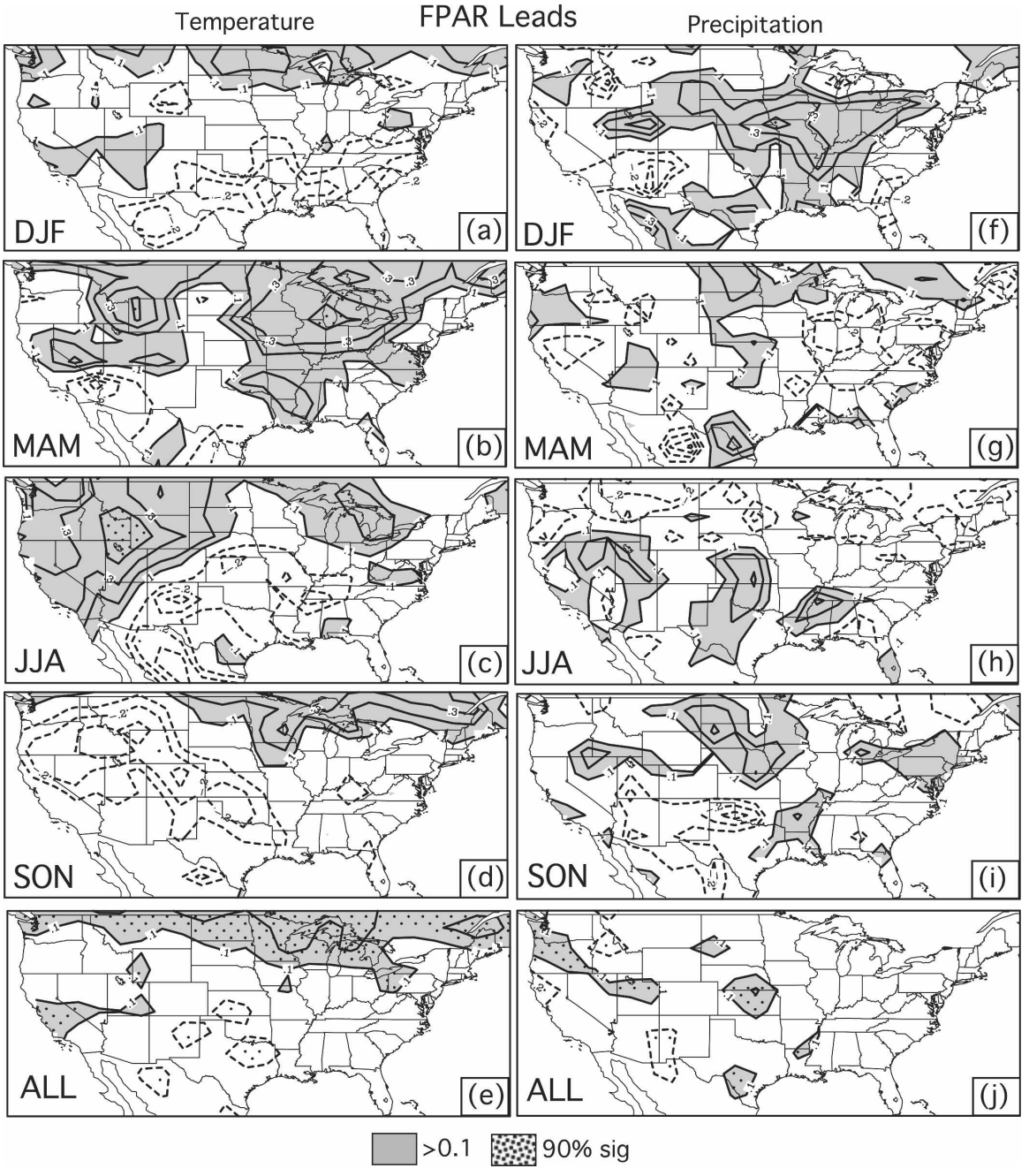

FIG. 12. As in Fig. 10 except FPAR leads the atmospheric variables by one month. These correlations suggest vegetation forcing on the atmosphere.

The substantial temperature forcing on FPAR in spring and FPAR forcing on temperature in autumn reflects the findings of Liu et al. (2006) for eastern Siberia. Precipitation fails to significantly force FPAR in Wisconsin during any season (also Fig. 10). The lead–lag correlations between FPAR and precipitation suggest a weak relationship in Wisconsin, although a negative correlation is identified between August–September FPAR and September precipitation ($p < 0.10$).

A similar analysis is performed for the central/northern Rockies (Fig. 14), which encompasses southern Idaho, southeastern Oregon, western Wyoming, northern Utah, and northern Nevada and is mostly shrubland and grassland. Correlations of monthly

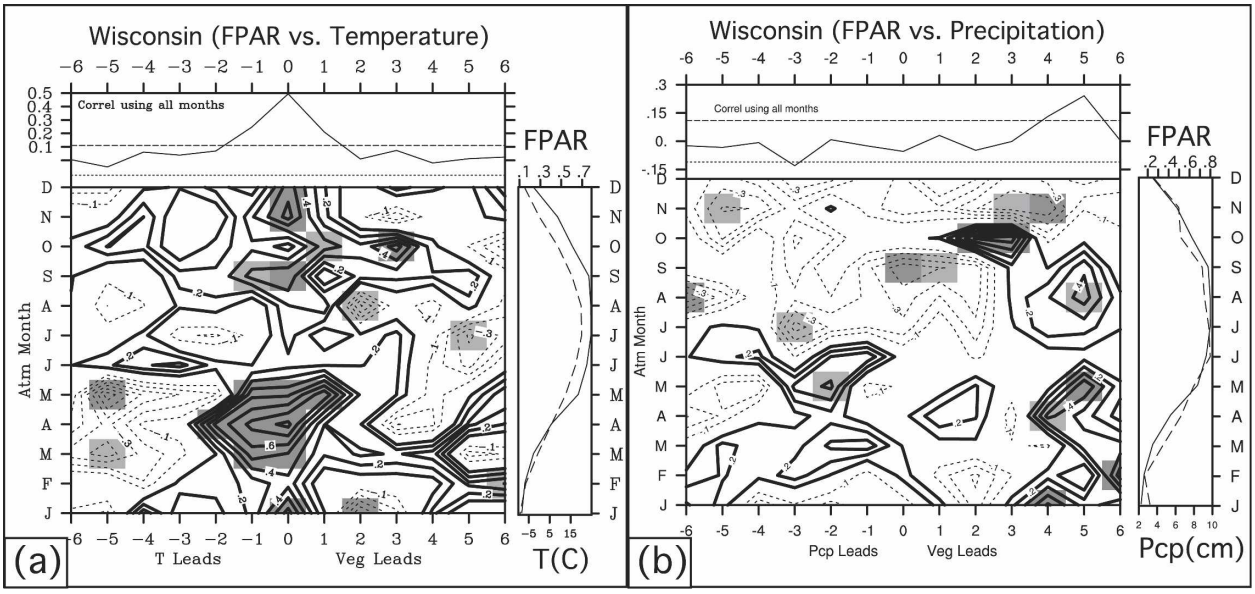

FIG. 13. (a) Lagged correlations between monthly anomalies of FPAR and surface airtemperature in Wisconsin (42.5°–47.5°N, 87.5°–92.5°W) for 1982–2000. (top) The annual mean of the FPAR–temperature lagged correlation with negative (positive) lags for temperature (FPAR) leading. The dash line indicates the 90% significance level. (bottom left) The seasonal evolution of the lagged correlation, with the months on the *y* axis designating the month for temperature. The light (dark) shading indicates the 90% (95%) significance level. The area-averaged climatological annual cycles of FPAR (solid) and temperature (dash) are also shown on the right panel. (b) As in (a) except for precipitation.

FPAR and temperature anomalies suggest a moderate instantaneous relationship along with significant temperature forcing at one-month lead and vegetation forcing at one-month lead ($p < 0.10$), with evidence of two-way vegetation–atmosphere forcing. Temperature forcing by FPAR is weaker across the central/northern Rockies than Wisconsin, particularly during spring. JJA FPAR anomalies are significantly positively correlated ($p < 0.10$) to late summer–early autumn (JAS) temperature in the central/northern Rockies. In general,

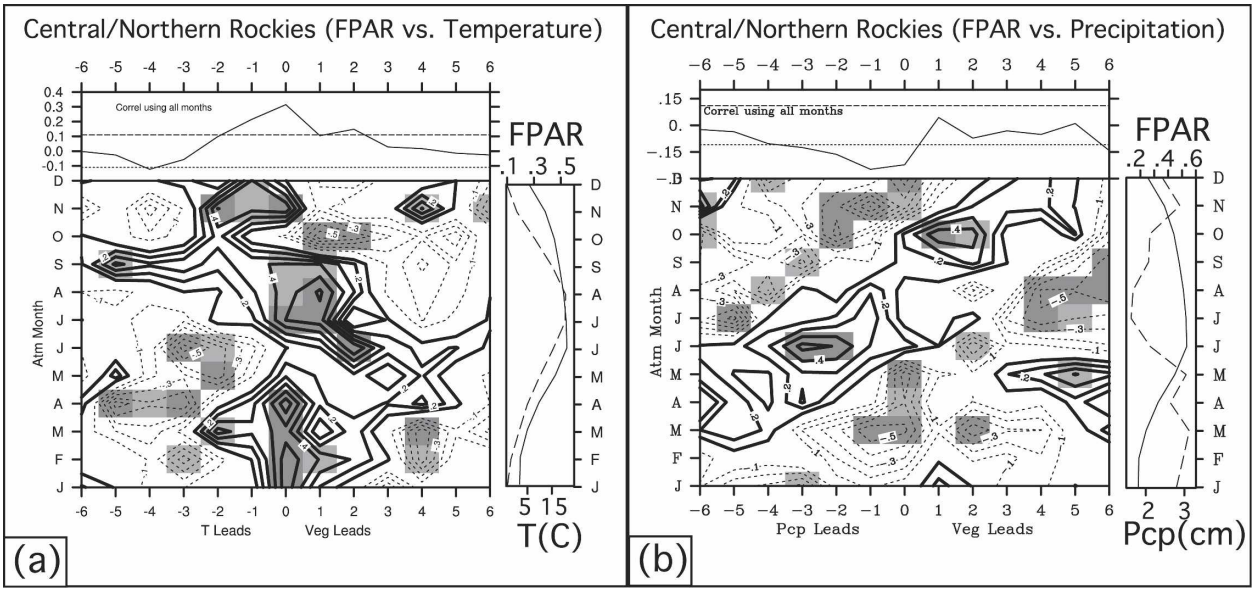

FIG. 14. As in Fig. 13 except for the central/northern Rockies (parts of OR, ID, WY, NV, and UT) (37.5°–45.0°N, 110.0°–120.0°W).

temperature forcing leads springtime FPAR, while FPAR forcing leads summer–autumn temperature in the central/northern Rockies (Fig. 14a). The negative correlations between FPAR and precipitation ($p < 0.10$) reflect the year-round inverse relationship between temperature and precipitation. FPAR anomalies during the late summer–autumn positively force October precipitation ($p < 0.05$), potentially through increased evapotranspiration (Fig. 1). Also, springtime FPAR is negatively correlated ($p < 0.05$) with precipitation in the subsequent late summer (dry season), although the mechanism is unclear. As with Wisconsin, there is generally not strong evidence of vegetation feedbacks on precipitation.

The two FPAR dipole centers are comprised mostly of shrubland and grassland (Fig. 15). FPAR at the northern center, centered on western South Dakota, is largely temperature driven, with a maximum correlation at zero lag. Correlations between FPAR and temperature anomalies are strongly positive from autumn to early spring ($p < 0.05$) but insignificant during summer. There is evidence of positive vegetation forcing on temperature in spring and late summer–early autumn. FPAR at the southern center, around Texas, is strongly determined by precipitation, with the maximum correlation when precipitation leads by one month. Correlations with precipitation leading are largest at lag 1 but statistically significant from lags 1–5, stressing the importance of the previous month's precipitation to supply sufficient soil moisture for plant growth. The southern center shows little evidence of significant vegetation feedbacks. Weak positive correlations with FPAR leading precipitation during spring reflect the findings for the Sahel by Liu et al. (2006), although the Sahel's correlations are statistically significant ($p < 0.10$); in both cases, positive FPAR anomalies support increased precipitation during the dry season, likely through enhanced evapotranspiration. At the southern center, FPAR imposes a weak negative forcing on growing season temperatures.

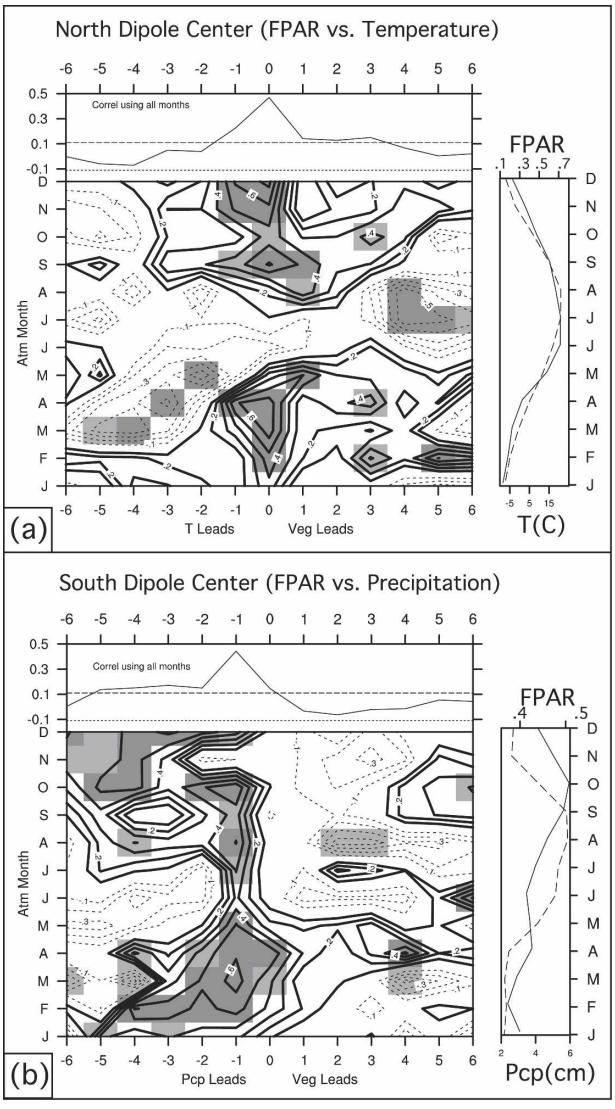

FIG. 15. As in Fig. 13 except for (a) the north dipole center (40.0°–50.0°N, 97.5°–110.0°W) (temperature) and (b) the south dipole center (25°–35°N, 97.5°–110.0°W) (precipitation).

6. Feedback parameters

The feedback parameter described in section 3 is computed for all months and individual seasons to assess the magnitude of the impact of FPAR on surface air temperature (Fig. 16). Across the northern United States this feedback parameter is most positive, approximately 1°–2°C $(0.1\ \text{FPAR})^{-1}$. A weaker, negative feedback parameter of −0.2° to −1°C $(0.1\ \text{FPAR})^{-1}$ characterizes the croplands of the south-central United States, where FPAR positively forces precipitation. The separation between positive and negative feedback parameter for all months approximately follows the 12°C isotherm with the most positive forcing on temperature in the coldest regions. The forcing on temperature is strongest and most positive in MAM and JJA, averaging 1.2°C $(0.1\ \text{FPAR})^{-1}$ across the United States; this feedback parameter is only 0.3°C $(0.1\ \text{FPAR})^{-1}$ in DJF and close to zero in SON, due to nearly equal areas of feedbacks with opposite signs. During MAM, the positive vegetation forcing on temperature is locally weaker over the prairie than over croplands and forests.

The percent variance in temperature attributed to forcing from FPAR is shown in Fig. 16, based on multiplying the feedback parameter squared by a ratio of FPAR variance to temperature variance and converting

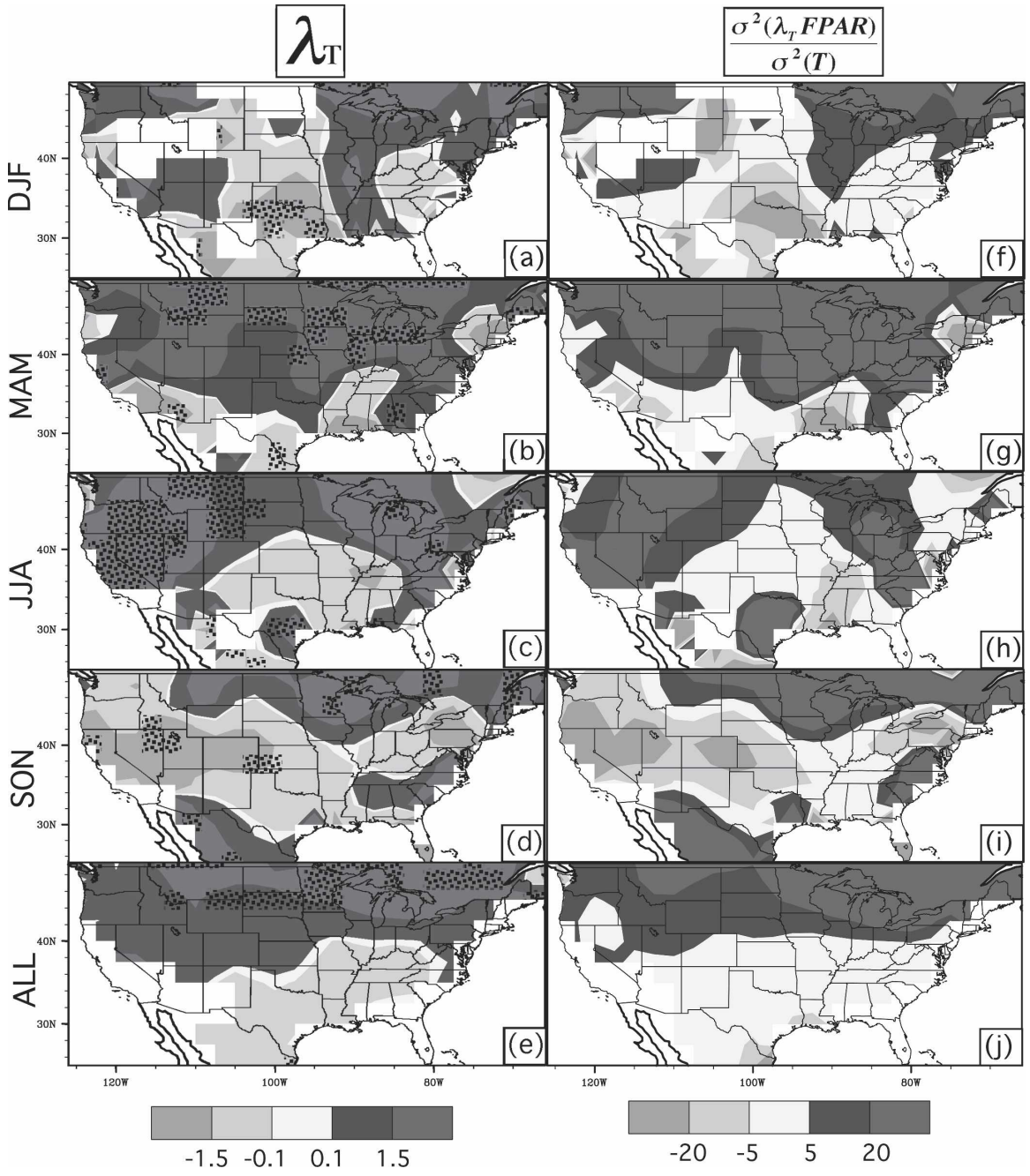

FIG. 16. (a)–(e) Vegetation feedback parameter [°C (0.1 FPAR)$^{-1}$] for monthly temperature anomalies and (f)–(j) percent explained variance of the feedback-induced variability (computed as the ratio of the variance of the feedback to the total temperature variance), both by season and for all months: dotted pattern indicates $p < 0.10$; regions with very small temperature autocorrelations are masked out.

to percentage. Across all months, this percentage is mostly 1%–10% south of 43°N but reaches 10%–50% across the upper Midwest and North. The feedback-induced variance accounts for the largest percentage of monthly temperature variance in MAM (30%), particularly over the Corn Belt and the northern United States. During JJA, the vegetation parameter for temperature is negative (though not significant) over the southern croplands and the Mississippi River valley; this hints at a possible feedback whereby increased vegetation in this region could lower the air temperature either by increasing latent heat flux or by increasing

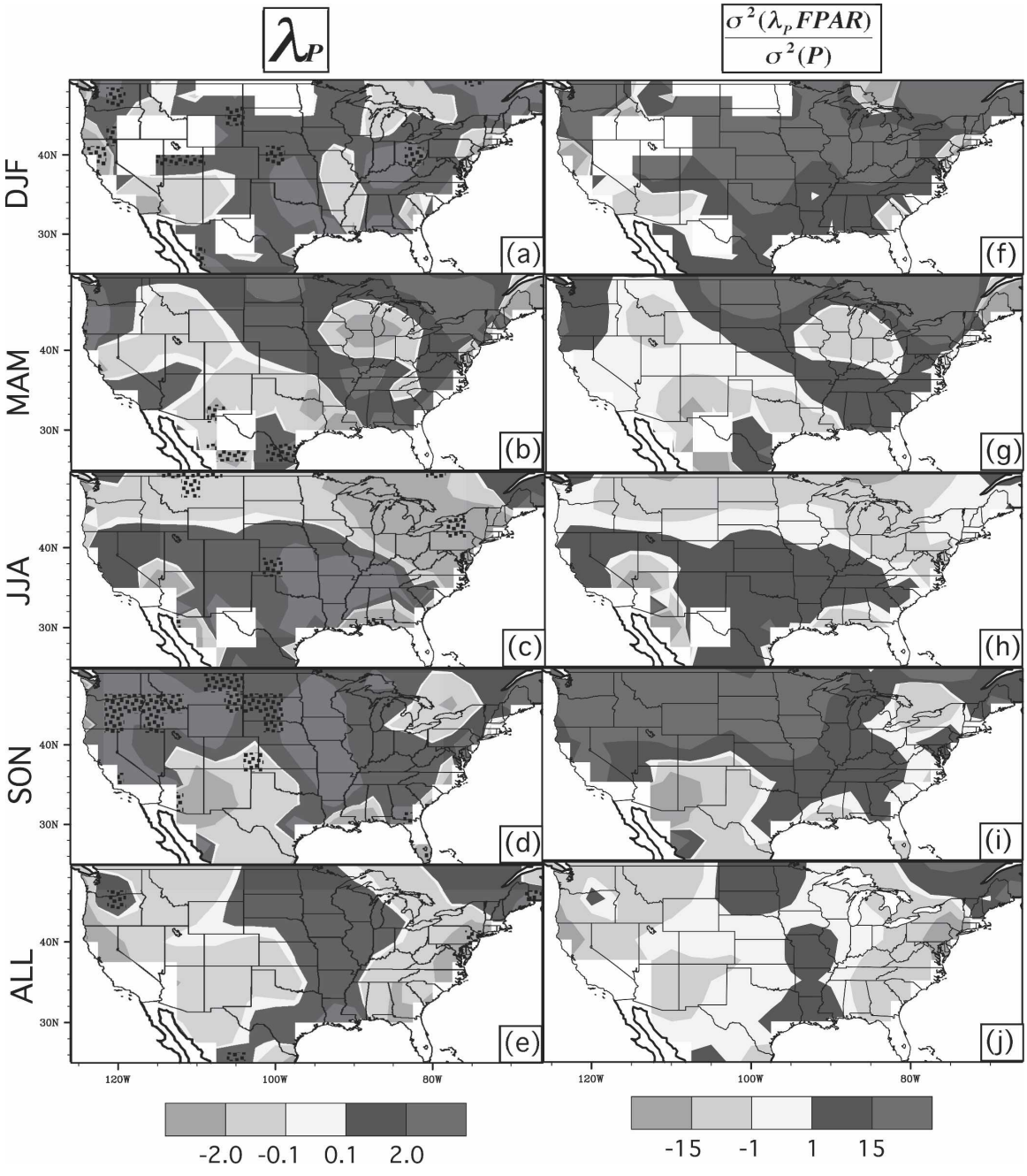

FIG. 17. As in Fig. 16 but for precipitation: units of the feedback parameters in (a)–(e) are cm month^{-1} (0.1 FPAR)$^{-1}$.

precipitation and consequently reducing surface solar radiation. Similarly, Snyder et al. (2004) concluded, using CCM3–IBIS, that the removal of the boreal forest produced the largest temperature signal globally and the removal of grasslands/steppe resulted in summertime warming and drying in central United States.

While numerous modeling studies have suggested that an increase in vegetation leads to cooling during summer (e.g., Bounoua et al. 2000), some have suggested similar vegetation impacts on temperature to those computed here. In a simulation with the boreal forest removed, Bonan et al. (1992) found year-round cooling that maximized in spring. The snow albedo effect was responsible for the cooling in winter and the transition seasons, while Bonan et al. (1992) attributed most of the summertime cooling to interactive SSTs and sea ice feedbacks. The present observational study agrees with the sign of this feedback during summer,

with increasing FPAR corresponding to increasing temperature across much of the United States. Bonan et al. (1992) proposed that increased summertime vegetation lowers the albedo and results in warming. Both Wohlfahrt et al. (2004) and Ganopolski et al. (1998) simulated positive vegetation forcing on temperature in the midhigh latitudes.

In an observation-based statistical analysis, Kaufmann et al. (2003) concluded that an increase in NDVI over North America results in significant warming during DJF and MAM, in agreement with the present study. They found that a NDVI increase in JJA produced weak cooling over North American forests; yet the present study concluded that increasing vegetation produced warming across much of North America except the southern United States. Kaufmann et al. (2003) did find that an increase in NDVI over broadleaf deciduous forests resulted in warming across all seasons in North America.

Figure 17 presents the vegetation feedback parameter for precipitation across all months and for each season, along with the percent variance in monthly precipitation associated with monthly FPAR feedbacks. The influence of FPAR on precipitation appears to be weak on these time scales, although stronger signals are noted during individual seasons. Few areas in Fig. 17 achieve statistical significance ($p < 0.10$) and, since the amount of significant areas is generally less than 10%, their significance might be the result of chance and therefore not statistically valid. Across all months, FPAR surprisingly exhibits a weak negative forcing on precipitation of -0.6 cm month^{-1} (0.1 FPAR)$^{-1}$ when averaged across the United States owing to the presence of vast areas with both positive and negative feedbacks. The feedback parameter is negative across the western shrublands/grasslands and eastern forests. This area of negative forcing on precipitation includes the region of winter wheat across western Kansas and Oklahoma, the Texas panhandle, and eastern Colorado.

Over the agricultural areas with corn and soybeans, which extend across the Corn Belt, northern plains, and Mississippi River valley, a positive feedback parameter of 0.05–2 cm month^{-1} (0.1 FPAR)$^{-1}$ is computed. It is likely that increased crop growth over this region enhances evapotranspiration and precipitation; summertime corn and soybean crops should be a greater source of evapotranspiration than winter wheat. Crop irrigation in the lower Mississippi River valley potentially contributes positive feedback on precipitation (Fig. 17e) (Rosenan 1963; Schickedanz 1976).

Although the mean feedback parameter for precipitation is negative across the United States, there are regions of substantial positive forcing [exceeding 2–4 cm month^{-1} (0.1 FPAR)$^{-1}$] during individual seasons and most regions that achieve statistical significance exhibit positive forcing. SON is characterized by the most positive vegetation feedback parameter, averaging $+0.9$ cm month^{-1} (0.1 FPAR)$^{-1}$. During JJA, the mean feedback parameter is -0.6 cm month^{-1} (0.1 FPAR)$^{-1}$, largely due to a strong negative forcing of -2 to -4 cm month^{-1} (0.1 FPAR)$^{-1}$ across the Northeast and upper Midwest and moderate negative forcing of -0.05 to -2 cm month^{-1} (0.1 FPAR)$^{-1}$ across the remaining northern United States. The positive feedback parameter for temperature and negative for precipitation during JJA over the former region suggests a warming and drying effect from increased FPAR within this area of mixed needleleaf and deciduous tree cover. W05 identified the northern grasslands/steppe (40°–50°N, 100°–115°W) as a key region of positive causal relationship from NDVI to temperature and negative causal relationship from NDVI to precipitation during the growing season. The present study's analysis of JJA produces similar results for this region, with mean feedback parameters of $+1.1$°C (0.1 FPAR)$^{-1}$ and -0.4 cm month^{-1} (0.1 FPAR)$^{-1}$; however, in the transition seasons strong positive forcing of FPAR on precipitation is also found. Local regions of positive vegetation influence on precipitation, averaging 1–4 cm month^{-1} (0.1 FPAR)$^{-1}$, overlap the winter wheat crops of the south central United States in DJF and spring wheat crops of the northern plains in MAM.

Monthly FPAR variance explains the largest percentage of precipitation variance during DJF, averaging 24% across the United States and exceeding 50% in the central prairie. During JJA, this percentage is under 10% nearly everywhere across the country with negative forcing on precipitation to the north of approximately 42°N and positive to the south. During MAM, the positive FPAR forcing over the southeast Canadian boreal forest and the spring wheat belt of the northern prairie explains 25%–50% of the precipitation variance. A similar percentage of variance is explained by positive FPAR forcing during SON from the northern Rockies into the western Corn Belt. The feedback parameter likely inflates the explained variance by including some effects from soil moisture and other external influences.

Based on the feedback parameters, the impact of vegetation is strongest on temperature during MAM and on precipitation in SON across the United States. Vegetation can mask high snow albedos and induce warming, while crops at harvest time are potentially significant sources of evapotranspiration and can enhance precipitation. For most of the country, vegetation

feedback parameters for precipitation fail to achieve statistical significance.

GCMs generally simulate a positive vegetation feedback on precipitation, with an increase in vegetation cover producing enhanced evapotranspiration and leading to increased precipitation, which then can increase vegetation amount (Shukla and Mintz 1982; Nobre et al. 1991; Kutzbach et al. 1996; Kleidon et al. 2000; Bonan 2002). However, W05 concluded that observed increases in vegetation lead to decreased precipitation during the NH growing season. They suggested that increased vegetation cover enhances evapotranspiration, which can reduce soil moisture (Adegoke 2000; Heck et al. 2001). The additional moisture in the atmosphere column can be transported away by the atmospheric circulation, resulting in a net loss of soil moisture from that region. The stomata close in response to drier soil and thereby reduce water flux into the atmosphere, leading to diminished precipitation and higher temperatures (Bonan 2002). Similarly, the present observational analysis found that the local impact of FPAR on precipitation is spatially inhomogeneous and relatively weak although, during JJA and for the yearly average, increased FPAR led to reduced precipitation for the United States, consistent with the results of W05. It is possible that increased vegetation may induce increased precipitation on a different time scale or that the transpired water is transported downstream by the atmospheric circulation, though we note that some caution should be applied in interpreting these results as the feedback parameter for precipitation is only statistically significant locally during JJA.

To test the robustness of the results, the lead/lag correlations and feedback parameters are also computed using the University of Delaware surface air temperature (Willmott and Robeson 1995) and the Global Precipitation Climatology Project (GPCP) (Huffman et al. 1997) datasets. The FPAR feedbacks agree quite well with those computed from the NCEP–NCAR reanalysis and Xie–Arkin datasets, with some differences noted spatially. The feedback estimates appear to be robust and not dataset dependent.

7. Conclusions

This study is the first to quantify observed vegetation feedbacks over the United States. Analogous to SSTs, FPAR typically has a persistence of a few months, longer than the atmosphere, and can interact with the atmosphere via several possible feedback mechanisms. Instantaneous correlations show that temperature is a significant control of FPAR for much of the United States, particularly in MAM. Unlike temperature, correlations between FPAR and precipitation anomalies are larger when the atmospheric variable leads by one month. Much of the prairie has a statistically significant correlation between JJA FPAR anomalies and precipitation anomalies from the previous month. The largest interannual FPAR variability occurs over the central U.S. prairie where a north–south dipole is identified. Correlations with FPAR leading by one month suggest a positive influence of vegetation on temperature over the upper Midwest in MAM and northern Rockies in JJA. An increase in FPAR produces both decreased surface albedo and increased latent heat flux; the former increases temperature and the latter decreases temperature. This study suggests that the albedo feedback is stronger since increases in FPAR generally lead to higher temperatures. Correlations fail to identify statistically significant feedbacks of FPAR on precipitation.

In addition to lead–lag correlations, Liu et al. (2006) computed a statistical feedback parameter to relate global satellite-based FPAR and observed temperature and precipitation. The present study continues this methodology and focuses on the United States, quantifying the influence of monthly FPAR on temperature and precipitation. The mean vegetation feedback parameters for temperature and precipitation average $0.9°C\ (0.1\ FPAR)^{-1}$ and $-0.6\ cm\ month^{-1}\ (0.1\ FPAR)^{-1}$, respectively, across all months. Increases in FPAR therefore result in net warming and drying, though the effect of FPAR on precipitation is weaker than for temperature and the feedback parameter for precipitation is not generally found to be statistically significant. The mean feedback parameter for temperature is most positive during MAM and JJA, with monthly FPAR anomaly variance explaining 30% of monthly temperature variance in MAM. Maps of vegetation feedback parameters for precipitation are spatially complex, although a positive forcing over the corn and soybean belt and negative forcing over the winter wheat belt are identified when computed across all months. W05 concluded that an increase in growing season NDVI in the NH leads to an increase in temperature and decrease in precipitation. This finding agrees with the present observational study but conflicts with most modeling studies.

Several limitations are identified in this observational study (Liu et al. 2006). FPAR data contain some biases, particularly a snow cover signal during the colder months. The data is limited to 19 years, thereby reducing the amount of statistical significant results achieved. The methodology is based on linear statistics, although the relationship between vegetation and climate is potentially nonlinear (Zhou et al. 2003). The approach

assumes vegetation interacts with the atmosphere locally, although the atmospheric circulation can transport transpired water to other regions (Zhang et al. 2003). Since the computed feedbacks might contain a signature of other slow changing climate components, such as soil moisture and SST, the feedback parameters in a sense represent an upper limit to the magnitude of vegetation feedbacks. We expect that a longer time series of data would likely yield more areas of statistically significant vegetation forcing on precipitation, although the local response might continue to be weak.

By quantifying the observed vegetation impacts on temperature and precipitation, the present regional study and the global analysis of Liu et al. (2006) establish a benchmark against which GCM-simulated feedbacks can be evaluated. Following the approach of Frankignoul et al. (2004), these estimated observed vegetation feedback parameters can be applied to evaluate model-simulated vegetation feedbacks and perform model intercomparisons, both globally and regionally.

Acknowledgments. This work is supported by NSF, DOE, and NASA. The authors thank Dr. Claude Frankignoul for his advice on significance testing. Comments from Dr. John Kutzbach and two anonymous reviewers were very helpful.

REFERENCES

Adegoke, J. O., 2000: Satellite-based investigation of land surface–climate interactions in the United States Midwest. Ph.D. thesis, The Pennsylvania State University, 162 pp.

Bazzaz, F. A., and E. D. Fajer, 1992: Plant life in a CO2-rich world. *Sci. Amer.,* **266,** 68–74.

Betts, A. K., and J. H. Ball, 1997: Albedo over the boreal forest. *J. Geophys. Res.,* **102,** 28 901–28 909.

Bonan, G., 2002: *Ecological Climatology: Concepts and Applications*. Cambridge University Press, 678 pp.

——, D. Pollard, and S. Thompson, 1992: Effects of boreal forest vegetation on global climate. *Nature,* **359,** 716–718.

Bounoua, L., G. J. Collatz, S. O. Los, P. J. Sellers, D. A. Dazlich, C. J. Tucker, and D. A. Randall, 2000: Sensitivity of climate to changes in NDVI. *J. Climate,* **13,** 2277–2292.

Brovkin, V., 2002: Climate–vegetation interaction. *J. Phys.,* **4,** 57–72.

Bryson, R. A., 1966: Air masses, streamlines and the boreal forest. *Geogr. Bull.,* **8,** 228–269.

Budyko, M. I., 1974: *Climate and Life*. Academic Press, 608 pp.

Buermann, W., 2002: The impact and response of vegetation to climate at interannual timescales. Ph.D. thesis, Boston University, 140 pp.

Collatz, G. J., J. T. Ball, C. Grivet, and J. A. Berry, 1991: Physiological and environmental regulation of stomatal conductance, photosynthesis and transpiration: A model that includes a laminar boundary layer. *Agric. For. Meteor.,* **54,** 107–136.

Czaja, A., and C. Frankignoul, 2002: Observed impact of Atlantic SST anomalies on the North Atlantic Oscillation. *J. Climate,* **15,** 606–623.

DeFries, R. S., J. R. G. Townshend, and M. C. Hansen, 1999: Continuous fields of vegetation characteristics at the global scale at 1km resolution. *J. Geophys. Res.,* **104,** 16 911–16 925.

——, M. C. Hansen, J. R. G. Townshend, A. C. Janetos, and T. R. Loveland, 2000: A new global 1-km dataset of percentage tree cover derived from remote sensing. *Global Change Biol.,* **6,** 247–254.

Eamus, D., and P. G. Jarvis, 1989: The direct effects of increase in the global atmospheric CO_2 concentration on natural and commercial temperate trees and forests. *Adv. Ecol. Res.,* **19,** 1–55.

Fitzjarrald, D. R., O. C. Acevedo, and K. E. Moore, 2001: Climatic consequences of leaf presence in the eastern United States. *J. Climate,* **14,** 598–614.

Foley, J. A., S. Levis, I. C. Prentice, D. Pollard, and S. L. Thompson, 1998: Coupling dynamic models of climate and vegetation. *Global Change Biol.,* **4,** 561–579.

Frankignoul, C., and K. Hasselmann, 1977: Stochastic climate models. Part II: Application to sea surface temperature anomalies and thermocline variability. *Tellus,* **29,** 289–305.

——, and E. Kestenare, 2002: The surface heat flux feedback, Part I: Estimates from observations in the Atlantic and the North Pacific. *Climate Dyn.,* **19,** 622–647.

——, A. Czaja, and B. L'Heveder, 1998: Air–sea feedback in the North Atlantic and surface boundary conditions for ocean models. *J. Climate,* **11,** 2310–2324.

——, E. Kestenare, M. Botzet, A. F. Carril, H. Drange, A. Pardaens, L. Terray, and R. Sutton, 2004: An intercomparison between the surface heat flux feedback in five coupled models, COADS and the NCEP reanalysis. *Climate Dyn.,* **22,** 373–388.

Gallimore, R., R. Jacob, and J. Kutzbach, 2005: Coupled atmosphere-ocean-vegetation simulations for modern and mid-Holocene climates: Role of extratropical vegetation cover feedbacks. *Climate Dyn.,* **25,** doi:10.1007/s00382-005-0054-z.

Ganopolski, A., C. Kubatzki, M. Claussen, V. V. Brovkin, and V. V. Petoukhov, 1998: The influence of vegetation–atmosphere–ocean interaction on climate during the mid-Holocene. *Science,* **280,** 1916–1919.

Gordon, H. R., J. W. Brown, and R. H. Evans, 1988: Exact Rayleigh scattering calculations for use with the Nimbus-7 coastal zone color scanner. *Appl. Opt.,* **27,** 2111–2122.

Granger, C. W. J., 1969: Investigating causal relations by econometric models and cross spectral models. *Econometrica,* **37,** 424–438.

Hartmann, D. L., 1994: *Global Physical Climatology*. Academic Press, 411 pp.

Heck, P., D. Luthi, H. Wernli, and C. Schar, 2001: Climate impacts of European-scale anthropogenic vegetation changes: A sensitivity study using a regional climate model. *J. Geophys. Res.,* **106,** 7817–7835.

Henderson-Sellers, A., K. McGuffie, and C. Gross, 1995: Sensitivity of global climate model simulations to increased stomatal resistance and CO_2 increases. *J. Climate,* **8,** 1738–1756.

Huete, A. R., 1988: A soil adjusted vegetation index (SAVI). *Remote Sens. Environ.,* **25,** 295–309.

Huffman, G. J., and Coauthors, 1997: The Global Precipitation Climatology Project (GPCP) combined precipitation dataset. *Bull. Amer. Meteor. Soc.,* **78,** 5–20.

Ichii, K., A. Kawabata, and Y. Yamaguchi, 2002: Global correla-

tion analysis for NDVI and climatic variables and NDVI trends: 1982 to 1990. *Int. J. Remote Sens.,* **23,** 3873–3878.

Jacobson, M. Z., 2004: The short-term cooling but long-term global warming due to biomass burning. *J. Climate,* **17,** 2909–2926.

Jones, H. G., 1983: *Plants and Microclimate*. Cambridge University Press, 323 pp.

Kalnay, E., and Coauthors, 1996: The NCEP/NCAR 40-Year Reanalysis Project. *Bull. Amer. Meteor. Soc.,* **77,** 437–471.

Kaufmann, R. K., and D. I. Stern, 1997: Evidence for human influence on climate from hemispheric temperature relations. *Nature,* **388,** 39–44.

——, L. Zhou, Y. Knyazikhin, N. V. Shabanov, R. B. Myneni, and C. J. Tucker, 2000: Effect of orbital drift and sensor changes on the time series of AVHRR vegetation index data. *IEEE Trans. Geosci. Remote Sens.,* **38,** 2584–2597.

——, ——, R. B. Myneri, C. J. Tucker, D. Slayback, N. V. Shabanov, and J. Pinzon, 2003: The effect of vegetation on surface temperature: A statistical analysis of NDVI and climate data. *Geophys. Res. Lett.,* **30,** 2147, doi:10.1029/2003GL018251.

Kleidon, A., K. Fraedrich, and M. Heimann, 2000: A green planet versus a desert world: Estimating the maximum effect of vegetation on the land surface climate. *Climatic Change,* **44,** 471–493.

Knapp, A. K., and M. D. Smith, 2001: Variation among biomes in temporal dynamics of aboveground primary production. *Science,* **291,** 481–484.

Kutzbach, J., G. Bonan, J. Foley, and S. P. Harrison, 1996: Vegetation and soil feedbacks on the response of the African monsoon to orbital forcing in the early and middle Holocene. *Nature,* **384,** 623–626.

Levis, S., G. B. Bonan, and C. Bonfils, 2004: Soil feedback drives the mid-Holocene North African monsoon northward in fully coupled CCSM2 simulations with a dynamic vegetation model. *Climate Dyn.,* **23,** 791–802.

Liu, Z., and L. Wu, 2004: Atmospheric response to North Pacific SST: The role of ocean–atmosphere coupling. *J. Climate,* **17,** 1859–1882.

——, M. Notaro, J. Kutzbach, and N. Liu, 2006: Assessing global vegetation–climate feedbacks from observations. *J. Climate,* **19,** 787–814.

Los, S. O., and Coauthors, 2000: A global 9-yr biophysical land surface dataset from NOAA AVHRR data. *J. Hydrometeor.,* **1,** 183–199.

——, G. J. Collatz, L. Bounoua, P. J. Sellers, and C. J. Tucker, 2001: Global interannual variations in sea surface temperature and land surface vegetation, air temperature, and precipitation. *J. Climate,* **14,** 1535–1549.

Loveland, T. R., and A. S. Belward, 1997: The IGBP–DIS global 1 km land cover data set, DISCover: First results. *Int. J. Remote Sens.,* **18,** 3291–3295.

——, B. C. Reed, J. F. Brown, D. O. Ohlen, J. Zhu, L. Yang, and J. W. Merchant, 2001: Development of a global land cover characteristics database and IGBP DISCover from 1-km AVHRR data. *Int. J. Remote Sens.,* **21,** 1303–1330.

Maurer, E. P., A. W. Wood, J. C. Adam, D. P. Lettenmaier, and B. Nijssen, 2002: A long-term hydrologically based dataset of land surface fluxes and states for the conterminous United States. *J. Climate,* **15,** 3237–3251.

McPherson, R. A., D. J. Stensrud, and K. C. Crawford, 2004: The impact of Oklahoma's winter wheat belt on the mesoscale environment. *Mon. Wea. Rev.,* **132,** 405–421.

Myneni, R. B., R. R. Nemani, and S. W. Running, 1997: Estimation of global leave area index and absorbed PAR using radiative transfer models. *IEEE Trans. Geosci. Remote Sens.,* **35,** 1380–1393.

——, C. J. Tucker, G. Asrar, and C. D. Keeling, 1998: Interannual variations in satellite-sensed vegetation index data from 1981 to 1991. *J. Geophys. Res.,* **103,** 6145–6160.

Nadelhoffer, K. J., A. E. Giblin, G. R. Shaver, and J. L. Laundre, 1991: Effects of temperature and substrate quality on element mineralization in six arctic soils. *Ecology,* **72,** 242–253.

Nobre, C. A., P. J. Sellers, and J. Shukla, 1991: Amazonian deforestation and regional climate change. *J. Climate,* **4,** 957–988.

Notaro, M., Z. Liu, R. Gallimore, S. J. Vavrus, J. E. Kutzbach, I. C. Prentice, and R. L. Jacob, 2005: Simulated and observed preindustrial to modern vegetation and climate changes. *J. Climate,* **18,** 3650–3671.

Penner, J. E., R. E. Dickinson, and C. A. O'Neill, 1992: Effects of aerosol from biomass burning on the global radiation budget. *Science,* **256,** 1432–1434.

Pielke, R., R. Avissar, M. Raupach, A. J. Dolman, X. Zhen, and A. S. Denning, 1998: Interactions between the atmosphere and terrestrial ecosystems: Influence on weather and climate. *Global Change Biol.,* **4,** 461–475.

Pollard, D., and S. L. Thompson, 1995: The effect of doubling stomatal resistance in a global climate model. *Global Planet. Change,* **10,** 1–4.

Ramankutty, N., and J. A. Foley, 1998: Characterizing patterns of global land use: An analysis of global croplands data. *Global Biogeochem. Cycles,* **12,** 667–686.

Risser, P. G., 1985: Grasslands. *Physiological Ecology of North American Plant Communities,* B. F. Chabot and H. A. Mooney, Eds., Chapman and Hall, 232–256.

Robinson, D. A., and G. Kukla, 1985: Maximum surface albedo of seasonally snow covered lands in the Northern Hemisphere. *J. Climate Appl. Meteor.,* **24,** 402–411.

Rosenan, N., 1963: Changes of climate. *Proc. Rome Symp.*, Paris, France, UNESCO/WMO, 67–73.

Schickedanz, P. T., 1976: Effect of irrigation on precipitation in the Great Plains. Illinois State Water Survey Final Rep. to NSF, RANN, 105 pp.

Schultz, P. A., and M. S. Halpert, 1993: Global correlation of temperature, NDVI and precipitation. *Adv. Space Res.,* **13,** 277–280.

Schwartz, M. D., 1992: Phenology and springtime surface-layer change. *Mon. Wea. Rev.,* **120,** 2570–2578.

——, 1996: Examining the spring discontinuity in daily temperature ranges. *J. Climate,* **9,** 803–808.

——, and T. R. Karl, 1990: Spring phenology: Nature's experiment to detect the effect of 'green-up' on surface maximum temperatures. *Mon. Wea. Rev.,* **118,** 883–890.

Shukla, J., and Y. Mintz, 1982: Influence of land-surface evapotranspiration on the Earth's climate. *Science,* **215,** 1498–1501.

Smith, E. L., 1937: The influence of light and carbon dioxide on photosynthesis. *J. Gen. Physiol.,* **20,** 807–830.

Snyder, P. K., C. Delire, and J. A. Foley, 2004: Evaluating the influence of different vegetation biomes on the global climate. *Climate Dyn.,* **23,** doi:10.1007/s00382-004-0430-0.

Sud, Y. C., J. Shukla, and Y. Mintz, 1988: Influence of land surface roughness on atmospheric circulation and precipitation: A sensitivity study with a general circulation model. *J. Appl. Meteor.,* **27,** 1036–1054.

Thonicke, K., S. Venevsky, S. Sitch, and W. Cramer, 2001: The role of fire disturbance for global vegetation dynamics: Cou-

pling fire into a global vegetation model. *Global Ecol. Biogeogr.,* **10,** 661–677.

Tian, Y., and Coauthors, 2004: Comparison of seasonal and spatial variations of leaf area index and fraction of absorbed photosynthetically active radiation from Moderate Resolution Imaging Spectroradiometer (MODIS) and Common Land Model. *J. Geophys. Res.*, **109,** D01103, doi:10.1029/2003JD003777.

Triacca, U., 2001: On the use of Granger causality to investigate the human influence on climate. *Theor. Appl. Climatol.,* **69,** 137–138.

von Storch, H., and F. W. Zwiers, 1999: *Statistical Analysis in Climate Research*. Cambridge University Press, 484 pp.

Walsh, J. E., W. H. Jasperson, and B. Ross, 1985: Influences of snow cover and soil moisture on monthly air temperature. *Mon. Wea. Rev.,* **113,** 756–768.

Wang, J., K. P. Price, and P. M. Rich, 2001: Spatial patterns of NDVI in response to precipitation and temperature in the central Great Plains. *Int. J. Remote Sens.,* **22,** 3827–3844.

——, P. M. Rich, and K. P. Price, 2003: Temporal responses of NDVI to precipitation and temperature in the central Great Plains, USA. *Int. J. Remote Sens.,* **24,** 2345–2364.

White, D. A., N. C. Turner, and J. H. Galbraith, 2000: Leaf water relations and stomatal behavior of four allopatric eucalyptus species in Mediterranean southwestern Australia. *Tree Physiol.,* **20,** 1157–1165.

Willmott, C. J., and S. M. Robeson, 1995: Climatologically aided interpolation (CAI) of terrestrial air temperature. *Int. J. Climatol.,* **15,** 221–229.

Wohlfahrt, J., S. P. Harrison, and P. Braconnot, 2004: Synergistic feedbacks between ocean and vegetation on mid- and high-latitude climates during the mid-Holocene. *Climate Dyn.,* **22,** 223–238.

Woodward, F. I., 1987: *Climate and Plant Distribution*. Cambridge University Press, 174 pp.

——, M. R. Lomas, and C. K. Kelly, 2004: Global climate and the distribution of plant biomes. *Philos. Trans. Roy. Soc. London,* **359B,** 1465–1476.

Wu, W., and R. E. Dickinson, 2004: Time scales of layered soil moisture memory in the context of land–atmosphere interaction. *J. Climate,* **17,** 2752–2764.

Xie, P., and P. A. Arkin, 1997: Global precipitation: A 17-year monthly analysis based on gauge observations, satellite estimates, and numerical model outputs. *Bull. Amer. Meteor. Soc.,* **78,** 2539–2558.

Zeng, X., P. Rao, R. DeFries, and M. C. Hansen, 2003: Interannual variability and decadal trend of global fractional vegetation cover from 1982 to 2000. *J. Appl. Meteor.,* **42,** 1525–1530.

Zhang, J., W. Dong, C. Fu, and L. Wu, 2003: The influence of vegetation cover on summer precipitation in China: A statistical analysis of NDVI and climate data. *Adv. Atmos. Sci.,* **20,** 1002–1006.

Zhou, L., R. K. Kaufmann, Y. Tian, R. B. Myneni, and C. J. Tucker, 2003: Relation between interannual variations in satellite measures of northern forest greenness and climate between 1982 and 1999. *J. Geophys. Res.,* **108,** 4004, doi:10.1029/2002JD002510.